Studies on the regulation of the DNA-binding activity of NPAS2, a mammalian circadian transcription factor

March, 2015

Department of Applied Life Science
Graduate School of Life and Environmental Science
Kyoto Prefectural University

Katsuhiro Yoshii

Contents

Abbreviations and Symbols

a.a.	amino acids
AMPK	adenosine monophosphate-activated protein kinase
bHLH	basic helix loop helix
BMAL1	brain and muscle ARNT like 1
CLOCK	circadian locomotor output cycles kaput
CO	carbon monoxide
CKI	casein kinase I
CRY	cryptochrome
DBP	D-site of albumin promoter binding protein
DTT	dithiothreitol
EDTA	ethylenediaminetetraacetic acid
EMS	electrophoretic mobility shift
FBXL	F-box and leucine-rich repeat protein
HAT	histone acetyltransferase
IPTG	isopropyl-β-D-thiogalactopyranoside
K_D	dissociation constant
NAAD	nicotinic acid adenine dinucleotide
NAD(H)	nicotinamide adenine dinucleotide (reduced form)
NADP(H)	nicotinamide adenine dinucleotide phosphate (reduced form)
NAMPT	nicotinamide phosphoribosyltransferase
NO	nitric oxide
NPAS2	neuronal PAS domain protein 2
OD	optical density
PER	period
PMSF	phenylmethanesulfonyl fluoride
ROR	retinoic acid receptor-related orphan receptor
SCN	suprachiasmatic nucleus
SIRT1	sirtuin 1

Chapter 1.

General introduction

Circadian rhythms are intrinsic mechanisms to adopt the environmental change occurred by the rotation of Earth, which are highly conserved in organisms ranging from cyanobacteria to humans. These rhythms have general characteristics that they autonomously continue in about 24 hour period even in constant darkness, have temperature-compensated periodicity and could be entrained by the environmental signals. In mammals, circadian rhythms control behavioral and physiological events such as the sleep-wake cycle, locomotor activity, body temperature, hormone release and metabolism. The master clock of mammalian circadian rhythms exists in the suprachiasmatic nucleus (SCN) which consists of twenty thousands of neuronal cells located at the hypothalamus, and it coordinates peripheral clocks that exist in most tissues such as lung, heart, liver, and kidney. Tissue destruction experiments revealed that the SCN clock was entrained by light input signal via retinohypothalamic tract, while restricted feeding experiments revealed that peripheral clocks were entrained by food intake signal in addition to the entrainment by the SCN clock [1].

At the molecular level, the breakthrough in the understanding of circadian clock was brought about by the discovery of clock genes defined as being necessary to generate normal circadian rhythms (Figure 1-1). It is currently known that the intracellular positive and negative transcriptional/translational feedback loops of clock genes and proteins generate the oscillations of circadian clocks [2-4]. As positive components of core loop, CLOCK and BMAL1 form a heterodimer to activate the transcription of various genes, including *Pers* and *Crys*, via E-box sequence in the promoter/enhancer region of these genes. Translated PERs and CRYs proteins, as the negative components of the clock machinery, form dimers or a large complex, are translocated into the nucleus, and eventually inhibit the transcriptional activity of CLOCK and BMAL1 [5-7].

In addition to this core loop, the orphan nuclear receptors RORs and Rev-erbs play important roles in the establishment of the more robust circadian clock. RORs and Rev-erbs, respectively, enhance and inhibit the transcription of *Clock* and *Bmal1* genes via RORE sites [8-11]. DBP and E4BP4, other clock proteins that are regulated their own transcription via E-box and RORE, respectively, make supporting loops by accelerating and inhibiting the transcription of clock genes via D-box sequence,

respectively. DEC1 and DEC2, members of the bHLH transcription factor superfamily, also form a supporting negative feedback loop for their own transcription via E-box sequence, while the transcription of *Dec1* and *Dec2* are also under the control of RORE [12].

Further, the circadian clock generated by these transcriptional feedback loops is affected by various environmental stimuli, including light, foods and hormones [13-15]. In response to light signal, glutamate and pituitary adenylate cyclase-activating polypeptide (PACAP) are released to SCN neuron, which is sequentially followed by the elevation of cAMP level in the SCN and the activation of cAMP response element-binding protein (CREB). An acute induction of *Per1* gene is caused by CREB via cAMP response element (CRE) in the *Per1* promoter and finally the phase shift of the clock is achieved [16]. On the other hand, intracellular concentrations of NAD^+ and heme, ligands of SIRT1 and Rev-erbs, respectively, impact on the circadian clock by the regulation of activities of these proteins, whereas the concentrations of these metabolites oscillate in a circadian fashion [17-19]. Moreover, glucocorticoid, a steroid hormone released from the cortex of the adrenal gland, activates glucocorticoid receptors that in turn bind to glucocorticoid response elements (GREs) in *Per1* and *Per2* genes, regulate their transcription, and reset the clocks in the peripheral tissues [20, 21]. It is also known that treatment with dexamethasone, a synthetic glucocorticoid, could synchronize the expression rhythms of several clock genes in individual cultured cells.

The clock proteins are also regulated at the post-transcriptional level, such as phosphorylation, sumoylation and ubiquitylation, to ensure the maintenance of circadian rhythms [22-29]. For example, AMP protein kinase (AMPK) and casein kinase Iε (CKIε) play essential roles in the turnover of CRY1 and PER1, respectively, by phosphorylating and decreasing their stability [25, 28]. In addition, a component of the Skp1-Cul1-F-box protein (SCF) ubiquitin ligases, F-box and leucine-rich repeat protein 3 (FBXL3) and β-transducin repeat-containing protein (β-TRCP), form SCF^{FBXL3} and $SCF^{\beta\text{-}TRCP}$ complexes to promote the ubiquitylation of phosphorylated CRY1 and PER1, respectively, and degrade these proteins via ubiquitin-proteasome pathway [25, 29].

Thus, various types of clock genes and proteins have been reported to date, and the understanding of their rigorous and concerted regulatory mechanisms for circadian clock is accelerating [30]. Furthermore, in recent years, accumulating evidences have demonstrated that the disruption of circadian clock causes or is related to many kinds of disease including mental disorder, diabetes, myocardial infarct, metabolic syndrome and cancer. Therefore, to establish the therapeutic methods of these diseases, further elucidation of molecular clockworks at the atomic level is required.

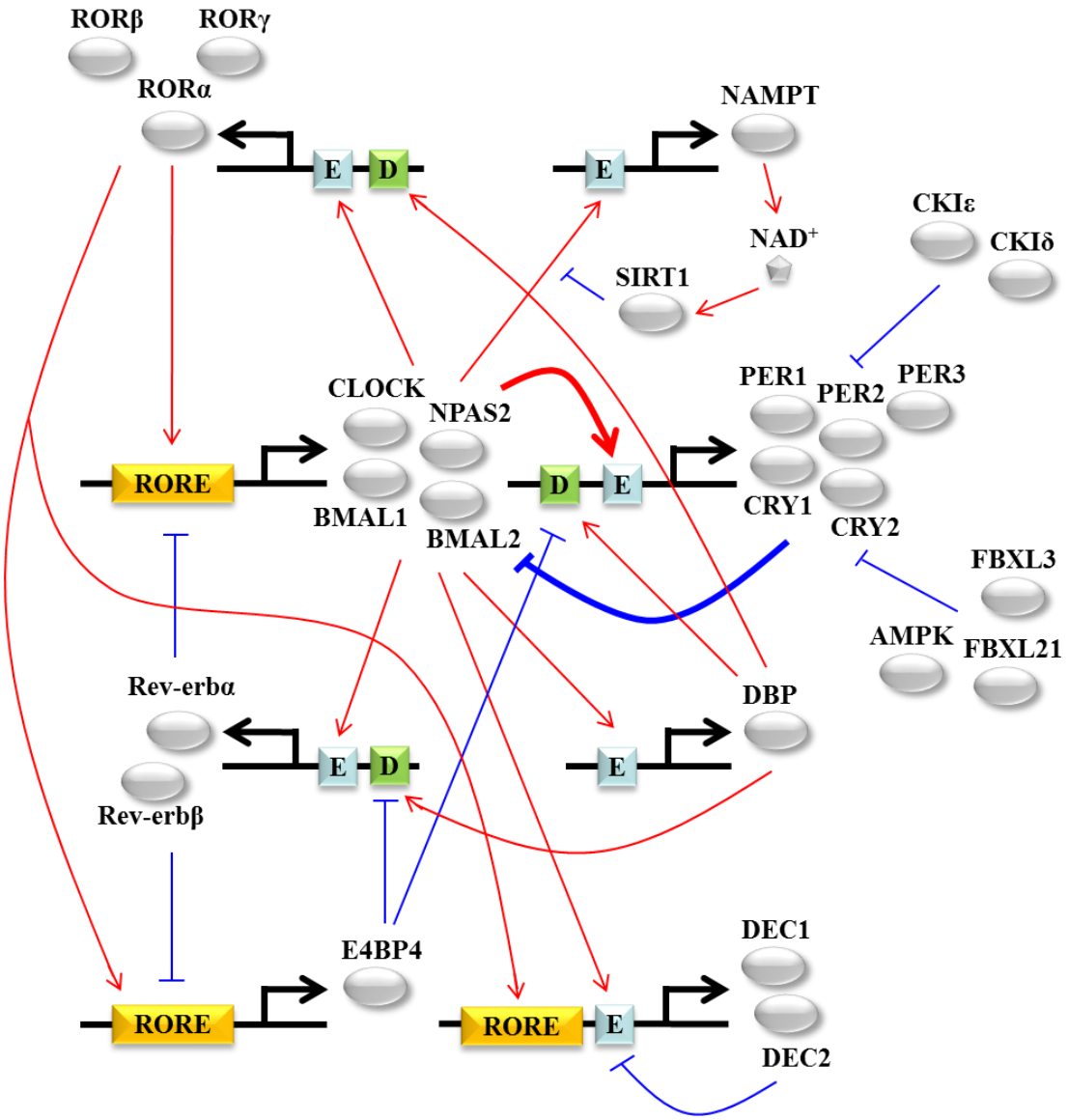

Figure 1-1. The circadian network of clock genes and proteins. The red and blue lines indicate positive and negative limbs, respectively. RORE, ROR binding element; E, E-box; D, D-box.

Neuronal PAS domain protein 2 (NPAS2), the subject of this thesis, is a core transcriptional activator regulating circadian rhythms. NPAS2 was originally isolated as a homolog of CLOCK in the mammalian forebrain [31, 32], but is also known to be expressed in the peripheral tissues [33, 34]. NPAS2, similar to CLOCK, forms a heterodimer with BMAL1 that binds to E-box sequences (CACGTG) or E-box like sequence (CACGTT) located in the regulatory regions of numerous clock genes and clock controlled genes to enhance their transcription [6, 32, 35]. Recently, chromatin immunoprecipitation sequencing (ChIP-seq) analyses have shown that there were about 2,300 of the DNA-binding sites for NPAS2 in murine liver, whereas about 4,600 and 5,900 sites for CLOCK and BMAL1, respectively [36]. Although the analyses of knockout mice revealed an overlapping role of CLOCK and NPAS2 in the circadian clock [33, 34], *Npas2*-deficient mice showed particular difficulty in their adaptability to food restriction and sleep homeostasis [33, 37]. A specific role of NPAS2 in metabolism has also been supported by the observations that single-nucleotide polymorphisms (SNPs) in *Npas2* have been linked to increased risks of cancer, metabolic syndrome and hypertension [38-40]. In addition, several genes involved in tumorigenesis were actually confirmed to be direct targets of NPAS2, and it was proposed that NPAS2 was a risk marker for cancer as well as a tumor suppressor [38, 40]. Therefore, it is particularly interesting to elucidate the regulation mechanism of NPAS2 function.

NPAS2 consists of a bHLH domain and two PAS domains (PASA and PASB) in the N-terminal half, and a transactivation domain in the C-terminal half. A bHLH domain is a protein structural motif which is characterized as a highly conserved DNA-binding domain and forms functional homodimer or heterodimer complexes with other bHLH proteins [41-43]. CACGTG (E-box) and CACGTT (E-box like) were demonstrated to be recognized by the bHLH domain of NPAS2, while in addition to these sequences, CACGNG and CATG(T/C)G were reported to be functional binding motifs for that of CLOCK [44]. On the other hand, PAS domains have now been observed in over 2,000 proteins, including kinases, transcription factors, ion channels and other enzymes that have diverse functions in signal transduction, protein-protein interactions and transcription [45, 46]. In NPAS2, each PAS domain binds heme as a prosthetic group with 1:1 stoichiometry, and the binding of CO and NO to the ferrous

heme regulates the DNA-binding activity of the NPAS2/BMAL1 heterodimer [47-49]. Since the binding affinity of CO to PASA-heme is about 10-fold greater than that to PASB-heme, the PASA domain is thought to act as a main gas sensor [47]. Additionally, previous study of resonance Raman spectra demonstrated that His119 and His171 were axial ligands of the ferric and ferrous heme in the isolated bHLH-PASA domain of NPAS2 [50].

Besides these features, it has also been suggested that the DNA-binding activity of NPAS2 is regulated by the intracellular redox state of NAD(P)H, although the mechanism remains unclear (Figure 1-2) [51]. In the chapter 2, therefore, to investigate the NAD(P)H interaction site of murine NPAS2, electrophoretic mobility shift (EMS) assays were performed using several truncation mutants of the NPAS2 bHLH domain. Furthermore, during these studies, it was also found that the complex formation of the NPAS2/BMAL1 heterodimer with DNA was affected by pH. In the chapter 3, the effects of pH on the DNA-binding activity and the transcriptional activity of NPAS2 were investigated in an EMS assay and a luciferase assay, respectively.

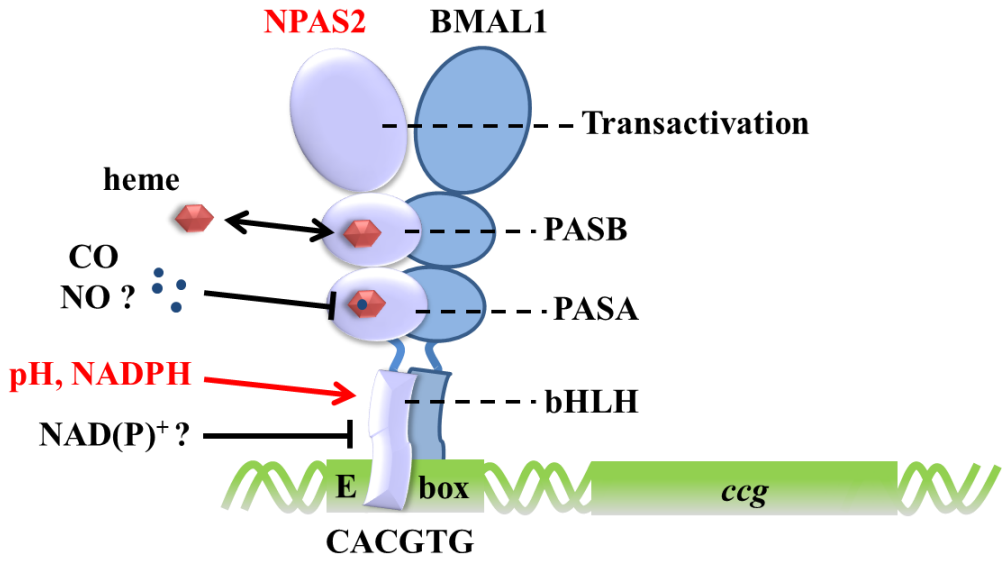

Figure 1-2. Proposed signals sensed by NPAS2. A heme binds PASA and PASB domains of NPAS2 reversibly. CO and NO bind ferrous heme of PAS domains of NPAS2, and CO-binding to the PASA ferrous heme inhibits the DNA-binding activity of NPAS2, whereas the effect of NO remains unclear. The effects of pH and NAD(P)H on the DNA binding activity of NPAS2 are described in this thesis. ccg, clock controlled genes.

Chapter 2.

Effects of NAD(P)H on the DNA-binding activity of NPAS2

2-1. Introduction

Circadian rhythms are fundamental mechanisms observed in almost all living organisms including cyanobacteria, drosophila, arabidopsis and humans. These rhythms control behavioral and physiological phenomenon, which are entrained by the daily light-dark cycle in a 24 hour period. In mammals, the master clock of circadian rhythms exists in the suprachiasmatic nucleus (SCN), and it coordinates peripheral clocks that exist in most tissues. At the molecular level, it is known that the intracellular positive and negative transcriptional/translational feedback loops of clock genes and proteins generate the oscillations of circadian clocks [1, 2, 4].

Neuronal PAS domain protein 2 (NPAS2) is a transcription factor associated with mammalian circadian rhythms, and it was originally identified as a homolog of CLOCK [32]. NPAS2 also forms a heterodimer with BMAL1 that binds to E-box sequences located in the promoter regions of *Per* and *Cry* genes and enhances their transcription. When PER and CRY proteins accumulate, they negatively regulate their own expression by inhibiting NPAS2/BMAL1 heterodimer. Although NPAS2 and CLOCK exhibit overlapping functions, NPAS2-deficient mice show particular difficulty in their adaptability to food restriction and sleep homeostasis [33, 37]. NPAS2 belongs to the bHLH-PAS superfamily and contains a bHLH domain, two PAS domains (PASA and PASB) and a transactivation domain. A bHLH domain is a basic DNA-binding domain that forms functional homodimer or heterodimer complexes with other bHLH proteins [41-43], while a PAS domain is a multifunctional protein domain that is contained in a large number of proteins [45, 46]. In NPAS2, each PAS domain binds heme as a prosthetic group, and the PASA domain acts as a gas sensor to regulate the DNA-binding activity of the NPAS2/BMAL1 heterodimer by CO and NO binding to the ferrous heme [47-50].

It was reported that NADH and NADPH enhanced the DNA-binding activity of the NPAS2/BMAL1 heterodimer, whereas NAD^+ and $NADP^+$ inhibited its activity, suggesting regulation by the redox state of the NAD cofactors [51]. These NAD cofactors are well known as essential electron carriers used in a huge number of metabolic pathways including glycolysis, TCA cycle, β-oxidation, and biosynthesis of

fatty acids, sterols and nucleotides. Since these processes is closely related to feeding, the regulation of circadian clock by the NAD cofactors is very interested finding as the evidence for the food entrainment of circadian rhythms, although it has already been accepted the idea that the circadian rhythms control the feeding behavior of animals.

In the report by *Rutter et al.*, the N-terminal 116 amino acids (a.a.) of murine NPAS2 and a.a. 75-126 of human BMAL1 were demonstrated to be sufficient for responsiveness to NAD(P)H [51]. However, their precise interaction sites and mechanisms remain unclear. Therefore, various truncated NPAS2 proteins were generated and electrophoretic mobility shift (EMS) assays were performed to examine how their DNA-binding activities were affected by NAD(P)H and its derivatives.

2-2. Materials and methods

2-2-1. Construction of expression plasmids

The expression plasmid for His-tagged murine NPAS2 bHLH-PASA (1-240 a.a.) was previously constructed [52]. The corresponding cDNA was cloned into the *Nde* I and *Sal* I sites of an *E. coli* expression vector, pET-28a(+) (Novagen), which introduced 6 × His-tag at the N-terminal of expressed proteins. To create the C-terminal truncation mutants of NPAS2 bHLH-PASA, NPAS2 bHLH (1-116 a.a.), bHLH (1-79 a.a.) and bHLH (1-61 a.a.), PCRs were performed using pET-28a(+) containing NPAS2 bHLH-PASA cDNA as the template. The primers used for PCR were 5’-CGGGATCCCATATGGACGAAGATGAGAAG-3’ as a sense primer for all mutants and 5’-CCCGTCGACCTAGAGAGGTGTGATAC-3’, 5’-CCCGTCGACCTAGAATGATGGCTTCC-3’ and 5’-CCCGTCGACCTATTCATTGTGTTTCTG-5’ as antisense primers for NPAS2 bHLH (1-116 a.a.), bHLH (1-79 a.a.) and bHLH (1-61 a.a.), respectively. The resulting products were subcloned into the *Nde* I and *Sal* I sites of pET-28a(+).

The expression plasmid for MBP-tagged murine BMAL1 bHLH-PASA-PASB (1-447 a.a.) was previously constructed [52]. The corresponding cDNA was cloned into the *Bam*H I and *Sal* I sites of an *E. coli* expression vector, pMAL-c2X (New England Biolabs), which introduced MBP-tag at the N-terminal of expressed proteins. To create BMAL1 bHLH-PASA (74-336 a.a.), PCR was performed using pMAL-c2X containing BMAL1 bHLH-PASA-PASB cDNA as the template. The primers used for PCR were 5’-CAGGATCCAGGGAGGCCCACAGTC-3’ as a sense primer and 5’-CGAGTCGACTATTTCACCCGTATTTCCCC-3’ as an antisense primer. The resulting product was subcloned into the *Bam*H I and *Sal* I sites of pMAL-c2X.

All of the desired constructs were confirmed by sequencing. The domain structures of these proteins are shown in Figure 2-1.

2-2-2. Expression and purification of the isolated bHLH-PASA and bHLH proteins of NPAS2

Expression and purification of the isolated bHLH-PASA or bHLH proteins of NPAS2 were performed essentially based on the method as described [49, 52]. *E. coli* BL21-CodonPlus (DE3)-RIL cells (Stratagene) were transformed with pET-28a(+) containing cDNA of NPAS2 bHLH-PASA or each cDNA of NPAS2 bHLH truncation mutants. The colonies were selected on a LB agar plate containing 30 μg/ml kanamycin and 35 μg/ml chloramphenicol. The cells were inoculated in TB medium containing the same antibiotics after preincubation of a single colony in LB medium and incubated at 37°C until the OD_{600} reached to 0.6. Then 0.05 mM IPTG was added into the medium to induce the protein expression after cooling down to 15°C and the culture continued for further 20 h with mild shaking.

The cells expressing each NPAS2 protein were collected by centrifugation and the cell extract was prepared by sonication in buffer A (50 mM sodium phosphate, pH 7.8, 50 mM NaCl, 10% glycerol, 2 μg/ml aprotinin, 2 μg/ml leupeptin, 2 μg/ml pepstatin A, 1 mM PMSF and 0.2 mM DTT). After ultracentrifugation, the supernatant was applied to a Ni-NTA agarose column (Qiagen) pre-equilibrated with buffer A. The column was washed sequentially with buffer A containing 20 mM and 70 mM imidazole for His-NPAS2 bHLH-PASA or 50 mM and 100 mM imidazole for His-NPAS2 bHLH truncation mutants. His-NPAS2 bHLH-PASA and truncation mutants were then eluted with buffer A containing 150 mM and 250 mM imidazole, respectively. The protein fractions were pooled, concentrated and applied to a Sephadex G-25 column (GE Healthcare) pre-equilibrated with buffer B (50 mM HEPES, pH 7.5, 10% glycerol and 1 mM DTT) to remove imidazole and for buffer exchange.

His-NPAS2 bHLH-PASA was prepared as holo-protein by reconstitution with two equivalents of hemin (2.5 mM stock in 0.01 N NaOH) and the apo-protein on ice for overnight. The excess hemin was removed by applying to a Sephadex G-25 column after the removal of insoluble fraction by centrifugation.

2-2-3. Expression and purification of the isolated bHLH-PASA-PASB and bHLH-PASA proteins of BMAL1

Expression and purification of the isolated bHLH-PASA-PASB or bHLH-PASA proteins of BMAL1 were carried out basically as described [52]. *E. coli* BL21-CodonPlus (DE3)-RIL cells were transformed with pMAL-c2X containing cDNA of BMAL1 bHLH-PASA-PASB or bHLH-PASA. The expression protocol was the same as that of His-NPAS2 proteins except the antibiotic was changed from 30 μg/ml kanamycin to 50 μg/ml ampicillin.

The cells expressing each BMAL1 protein were collected by centrifugation and the cell extract was prepared by sonication in buffer C (20 mM Tris-HCl, pH 7.4, 200 mM NaCl, 1 mM EDTA, 2 μg/ml aprotinin, 2 μg/ml leupeptin, 2 μg/ml pepstatin A, 1 mM PMSF and 2 mM DTT). After ultracentrifugation, the supernatant was applied to an Amylose Resin column (New England Biolabs) pre-equilibrated with buffer C. The column was washed sequentially with buffer C and buffer C containing 0.01 mM maltose. The MBP-tagged proteins were then eluted with buffer C containing 1 mM maltose. The protein fractions were applied to a Sephadex G-25 column pre-equilibrated with buffer B to remove maltose and for buffer exchange. The purified proteins were quickly frozen in liquid nitrogen and stored at -80°C until use.

2-2-4. EMS assay

The single-stranded oligonucleotides containing a canonical E-box sequence (5'-GGGGCGCCACGTGAGAGG-3' and 5'-GGCCTCTCACGTGGCGCC-3') were annealed and end-labeled with [^{32}P] dCTP (Japan Radioisotope Association) by Klenow enzyme (Takara) to use as an EMS probe. After the purification by ethanol precipitation, ^{32}P-labeled E-box probe was dissolved in TE buffer.

The DNA-binding reactions were performed for 30 min on ice in 6 μl of the reaction mixture (0.3 or 0.6 μM His-NPAS2, 0.6 μM MBP-BMAL1, 0.1 μM ^{32}P-labeled E-box, 50 mM HEPES, pH 7.5, 50 mM NaCl, 1.2 mM $MgCl_2$, 10% glycerol, 0.5% n-octyl-glycoside, 0.12 mg/ml BSA, 0.05 mg/ml poly-dI-dC (Sigma) and 2 mM DTT). To analyze the effects of NAD(P)H on the DNA-binding activity of NPAS2/BMAL1 heterodimer or BMAL1 homodimer, various concentrations of NAD(P)H were added to

the reaction mixture. In competition assays between NAD(P)H and its derivatives, the concentration of NAD(P)H was fixed at 2 mM and the derivatives were added to the reaction mixture at various concentrations. Because $NAD(P)^+$, nicotinic acid and NAAD had acidic pH values in aqueous solution, the stock solutions of these compounds were pH-adjusted to 7.5 just before the experiments.

The reaction mixtures were separated by electrophoresis on 5% (w/v) non-denaturing acrylamide gels in buffer D (20 mM Tris-acetate and 0.5 mM EDTA) for 2.5 h at 100 V and 4°C. After electrophoresis, the gels were dried and analyzed using a BAS-1800 II Image Analyzer (Fujifilm) with Multi Gauge V2.1. The binding data were analyzed with Igor Pro.

2-3. Results and discussion

2-3-1. Protein expression and purification

The domain structures of truncated proteins of NPAS2 and BMAL1 used in this chapter were shown in Figure 2-1. All of the purified proteins were analyzed by SDS-PAGE. Purified His-NPAS2 proteins were more than 95% purity, except for His-NPAS2 bHLH (1-79 a.a.), which was approximately 60% homogeneity with lower yield (Figure 2-2). These results suggest that NPAS2 bHLH (1-61 a.a.) has a more stable domain structure than bHLH (1-79 a.a.). Each of the bHLH proteins showed a typical α-helical structure in circular dichroism spectra, indicating that it was properly folded (Figure 2-3). As shown in Figure 2-4, the UV-vis absorption spectra of the ferric, ferrous and ferrous-CO complexes of His-NPAS2 bHLH-PASA were obtained as previously reported, confirming the structure of the PASA domain [50]. Purified MBP-BMAL1 proteins were more than 85% homogeneity as shown in lanes 5 and 6 of Figure 2-2.

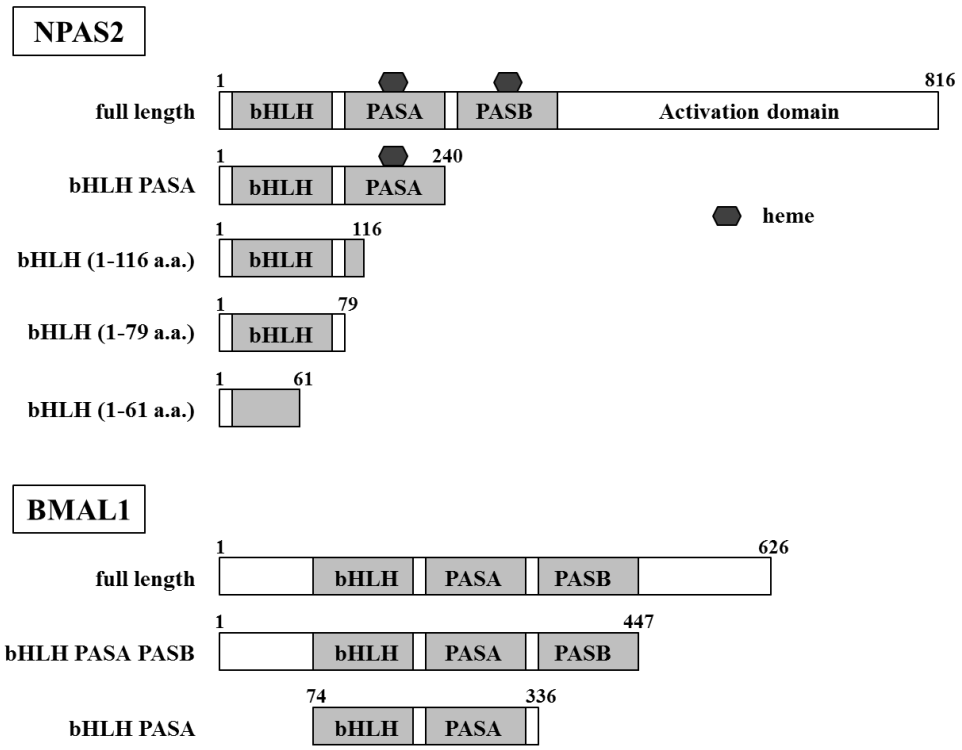

Figure 2-1. Domain structures of truncated NPAS2 and BMAL1 used in this chapter.

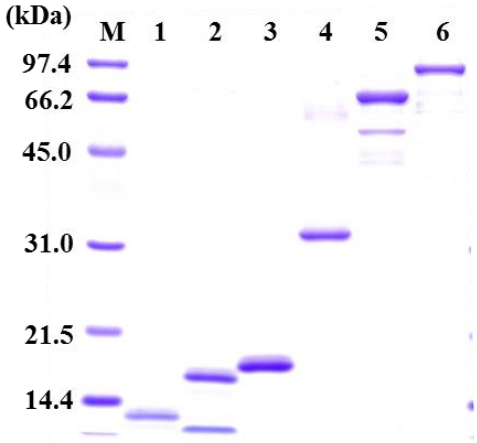

Figure 2-2. SDS-PAGE analysis of the purified proteins used in this chapter.
M; Molecular marker, 1; His-NPAS2 bHLH (1-61 a.a.),
2; His-NPAS2 bHLH (1-79 a.a.), 3; His-NPAS2 bHLH (1-116 a.a.),
4; His-NPAS2 bHLH-PASA (1-240 a.a.), 5; MBP-BMAL1 bHLH-PASA (74-336 a.a.),
6; MBP-BMAL1 bHLH-PASA-PASB (1-447 a.a.).

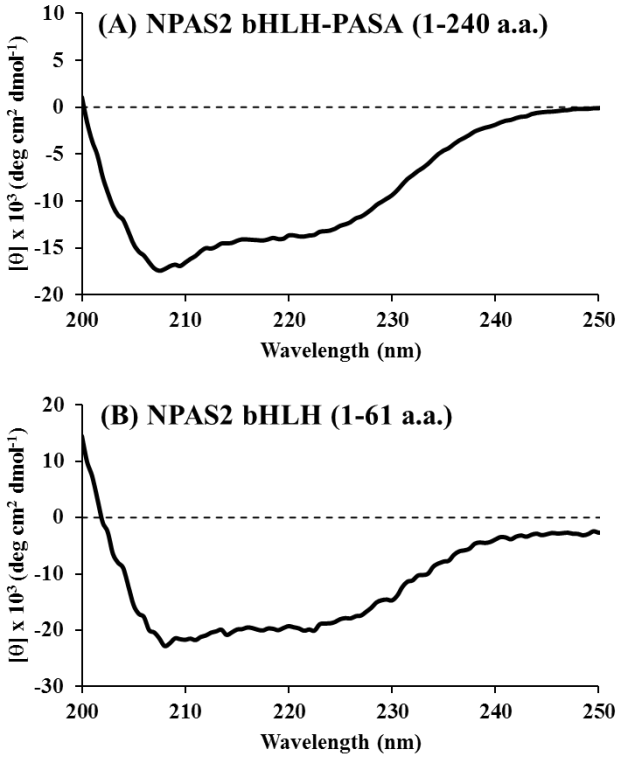

Figure 2-3. CD spectra of purified His-NPAS2 bHLH-PASA (1-240 a.a.) (A) and His-NPAS2 bHLH (1-61 a.a.) (B), in 100 mM Tris-HCl buffer (pH 7.5) containing 10% glycerol and 100 mM NaCl.

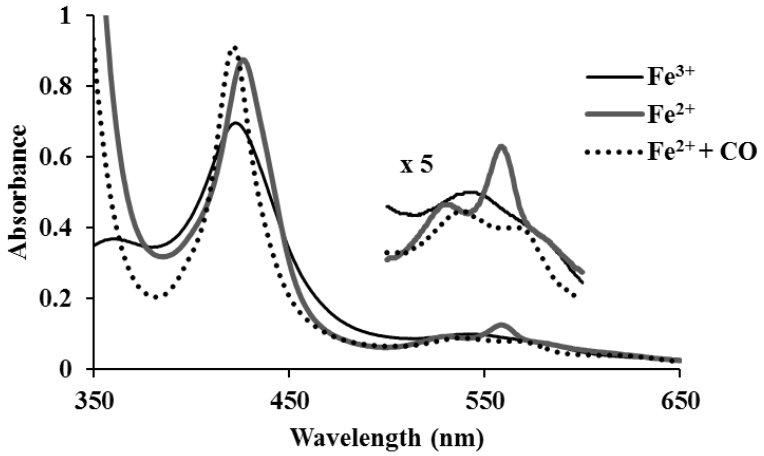

	Soret (nm)	visible (nm)
Fe(Ⅲ)	422	543.5
Fe(Ⅱ)	426.5	531, 558.5
Fe(Ⅱ) + CO	421.5	536, 567

Figure 2-4. The UV-vis absorption spectra of the ferric, ferrous and ferrous-CO complexes of His-NPAS2 bHLH-PASA, in 100 mM Tris-HCl buffer (pH 8.0) containing 10% glycerol and 1 mM DTT.

2-3-2. Effects of NAD(P)H on the DNA-binding activity of truncation mutants of NPAS2

To identify the interaction sites of NPAS2 with NADPH, the effects of NADPH on the DNA-binding activity of various truncation mutants of NPAS2 bHLH-PASA were examined in an EMS assay. As shown in Figure 2-5, two bands were observed when the ^{32}P-labeled E-box probe was incubated with both NPAS2 bHLH-PASA and BMAL1 bHLH-PASA-PASB proteins in the absence of NADPH. The addition of 5 mM NADPH resulted in decrease of the upper band and increase of the lower band. The estimated molecular sizes of BMAL1 homodimer and NPAS2/BMAL1 heterodimer are 186 kDa and 123 kDa, respectively, indicating that the upper and lower bands correspond to BMAL1 homodimer and NPAS2/BMAL1 heterodimer. The super-shift analysis using an anti-His-tag antibody confirmed that the lower band contained His-NPAS2 bHLH-PASA and corresponded to the NPAS2/BMAL1 heterodimer [52]. On the other hand, the complex of NPAS2 homodimer with ^{32}P-labeled E-box probe was not observed under experimental conditions used in this study as previously reported [52], although weak binding of holo-NPAS2 to the E-box DNA was observed under specific conditions by quartz crystal microbalance analyses [49]. As shown in Figure 2-6A, the DNA-binding activity of NPAS2/BMAL1 heterodimer was increased by the addition of NADPH in a dose-dependent manner. The EC_{50} of NADPH for NPAS2 bHLH-PASA (1-240 a.a.) was estimated to be 2.3 mM, consistent with the results for NPAS2 bHLH-PASA-PASB (1-416 a.a.) in Rutter *et al*. [51]. NADH also enhanced the DNA-binding activity of NPAS2/BMAL1 heterodimer with an EC_{50} value of 3.5 mM (Figure 2-7).

The His-NPAS2 bHLH truncation mutants were examined under the same conditions for NADPH effects. Each mutant of NPAS2 bHLH, NPAS2 bHLH (1-116 a.a.), bHLH (1-79 a.a.) and bHLH (1-61 a.a.), formed a heterodimer with BMAL1 that bound to ^{32}P-labeled E-box probe. The addition of NADPH enhanced their DNA-binding activities similarly to NPAS2 bHLH-PASA (Figure 2-6B, C and D). The EC_{50} of NADPH for NPAS2 bHLH (1-116 a.a.), bHLH (1-79 a.a.) and bHLH (1-61 a.a.) were 3.9, 3.6 and 2.1 mM, respectively. These results indicated that the N-terminal 1-61 amino acids of NPAS2 were sufficient for heterodimer formation with BMAL1 bHLH-PASA-PASB, E-box binding and the effect of NADPH. Similar results were

obtained with MBP-BMAL1 bHLH-PASA as shown in Figure 2-8. It was surprising that NPAS2 bHLH (1-61 a.a.) showed a response to NADPH because this mutant was estimated as the minimum size for a bHLH DNA-binding domain from a domain search (Figure 2-9). The EC_{50} value of NPAS2 bHLH (1-61 a.a.) was lower than those of the other truncation mutants, suggesting that the fragment could contain an interaction site for NADPH. It was also noticed that the addition of NPAS2 bHLH (1-61 a.a.) resulted in the drastic decrease of the complex of BMAL1 homodimer with ^{32}P-labeled E-box probe in the absence of NADPH. Similar results were obtained for NPAS2 bHLH (1-116 a.a.) and bHLH (1-79 a.a.), but not for NPAS2 bHLH-PASA (Figure 2-6). These results suggest that the heterodimer of NPAS2 bHLH and BMAL1 bHLH-PASA-PASB was more likely to be formed than the homodimer of BMAL1, but in the absence of NADPH, the affinity of the heterodimer to E-box was not enough to see as a retarded-band. Further experiments are needed to elucidate the precise kinetics of the NPAS2/BMAL1 heterodimer and BMAL1 homodimer formations and their DNA-binding affinities.

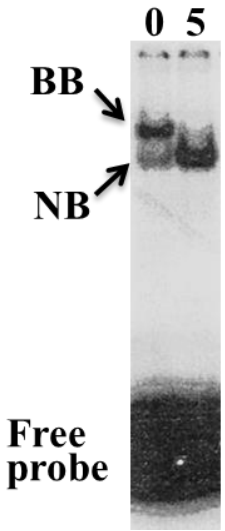

Figure 2-5. A typical autoradiograph of EMS assay-gel. NPAS2 bHLH-PASA (1-240 a.a.) and BMAL1 bHLH-PASA-PASB (1-447 a.a.) were used in the absence (0) and presence (5) of 5 mM NADPH. BB, BMAL1 homodimer with ^{32}P-labeled E-box probe; NB, NPAS2/BMAL1 heterodimer with the probe.

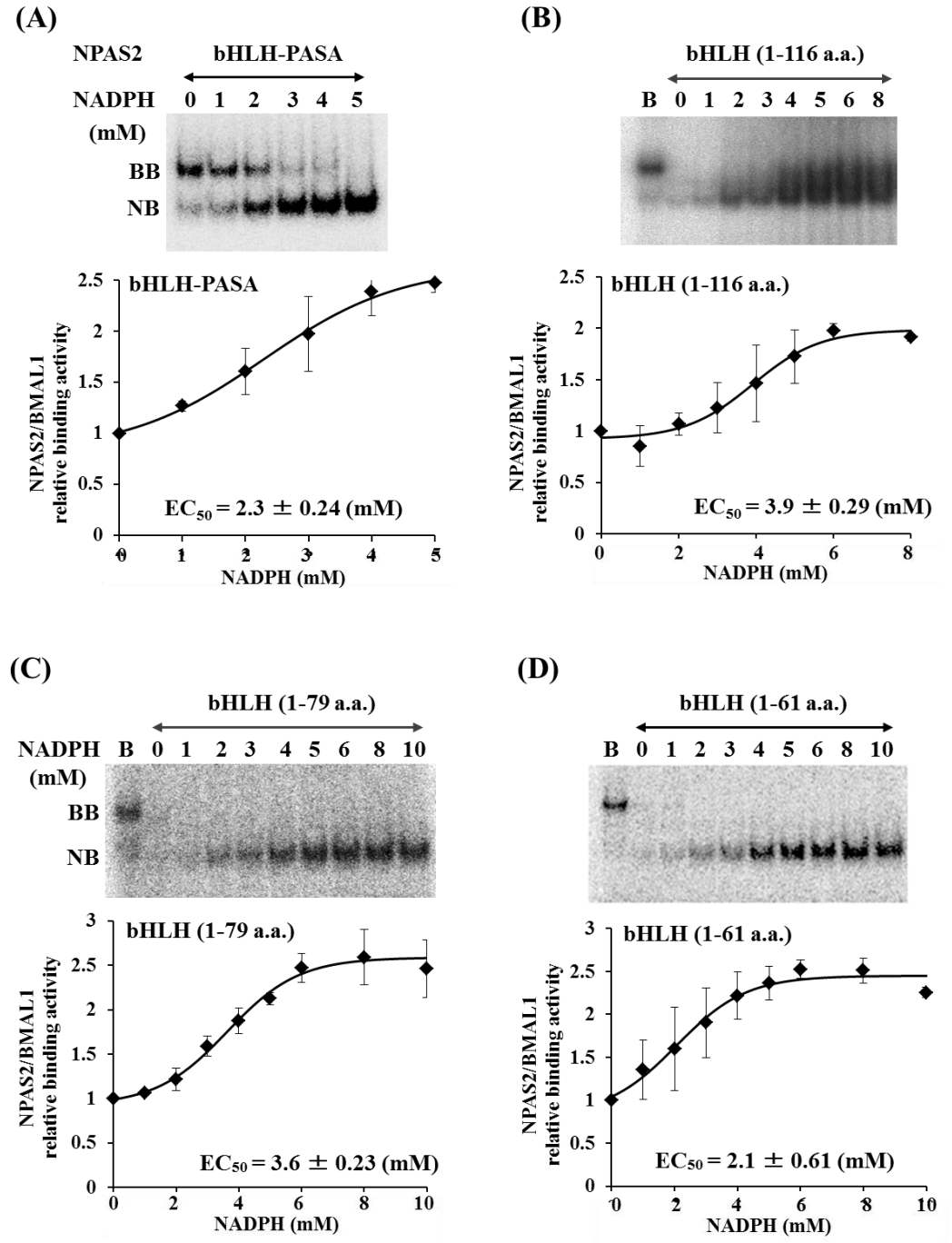

Figure 2-6. Effects of NADPH on the DNA-binding activity of NPAS2 bHLH-PASA and bHLH truncated mutants, with BMAL1 bHLH-PASA-PASB. The DNA-binding activities of NPAS2 bHLH-PASA (A), bHLH (1-116 a.a.) (B), bHLH (1-79 a.a.) (C) and bHLH (1-61 a.a.) (D) were analyzed in the presence of various amounts of NADPH. The label "B" at the top of the gel indicates an EMS assay in which BMAL1 protein was incubated with DNA in the absence of NPAS2. The DNA-binding activities of NPAS2/BMAL1 heterodimer were quantified by Multi Gauge V2.1 and represented

relative values normalized to the value obtained in the absence of NADPH. Each dot is the mean of at least three independent experiments ± SD. EC_{50} values were estimated from sigmoidal plots fitted to the data.

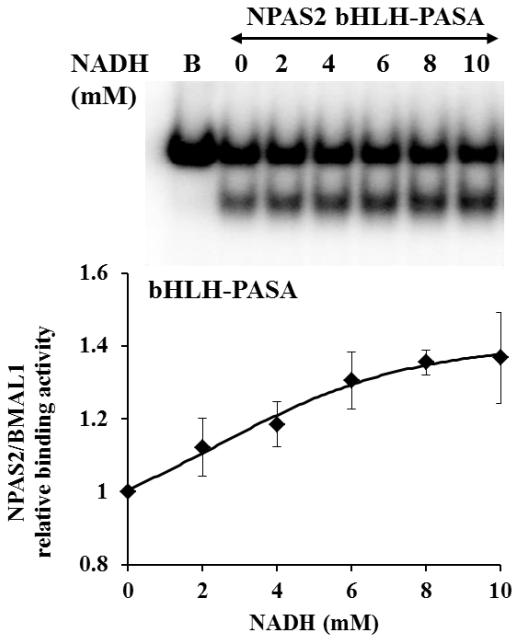

Figure 2-7. Effects of NADH on the DNA-binding activity of NPAS2 bHLH-PASA with BMAL1 bHLH-PASA-PASB. Experimental procedures were described in Figure 2-6.

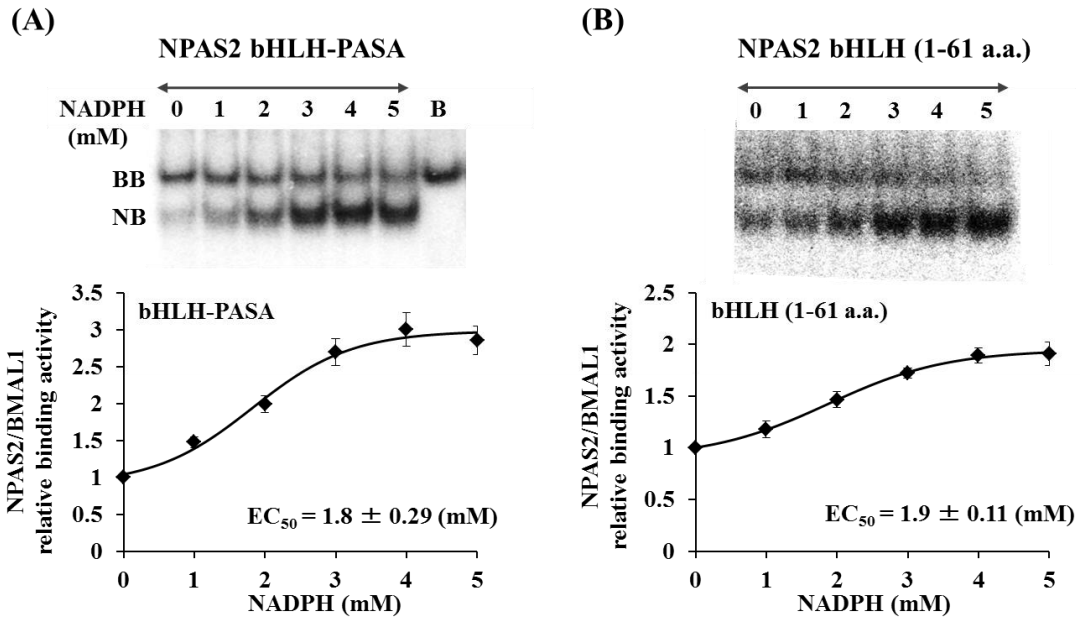

Figure 2-8. Effects of NADPH on the DNA-binding activity of NPAS2 bHLH-PASA (A) and bHLH (1-61 a.a.) (B), with BMAL1 bHLH-PASA. Experimental procedures were described in Figure 2-6.

Figure 2-9. Sequence alignment of the bHLH domains of NPAS2, CLOCK, and BMAL1. The secondary structure elements elucidated from the crystal structure of the CLOCK/BMAL1 heterodimer [53, 54] are shaded and marked.

2-3-3. Effects of NADPH on the DNA-binding activity of BMAL1 homodimer

Effects of NADPH on the DNA-binding activity of BMAL1 homodimer were examined by EMS assays using the purified bHLH-PASA-PASB and bHLH-PASA domains of BMAL1 in the absence of NPAS2. As shown in Figure 2-10, NADPH inhibited the DNA-binding activity of BMAL1 homodimer in a dose-dependent manner. The DNA-binding activities of BMAL1 bHLH-PASA-PASB and bHLH-PASA were 50% inhibited by addition of 7.6 and 8.4 mM NADPH, respectively. Interestingly, NADPH oppositely affected the DNA-binding activities of NPAS2/BMAL1 heterodimer and BMAL1 homodimer. The inhibition of the DNA-binding activity of BMAL1 homodimer may facilitate NPAS2/BMAL1 heterodimer formation at higher concentrations of NADPH. These results indicate that the enhancement of DNA-binding activity by NADPH was specific for NPAS2/BMAL1 heterodimer formation and/or the interaction between the heterodimer and E-box DNA. These results also suggest that the MBP-tag and BMAL1 protein were not sites for activation by NADPH.

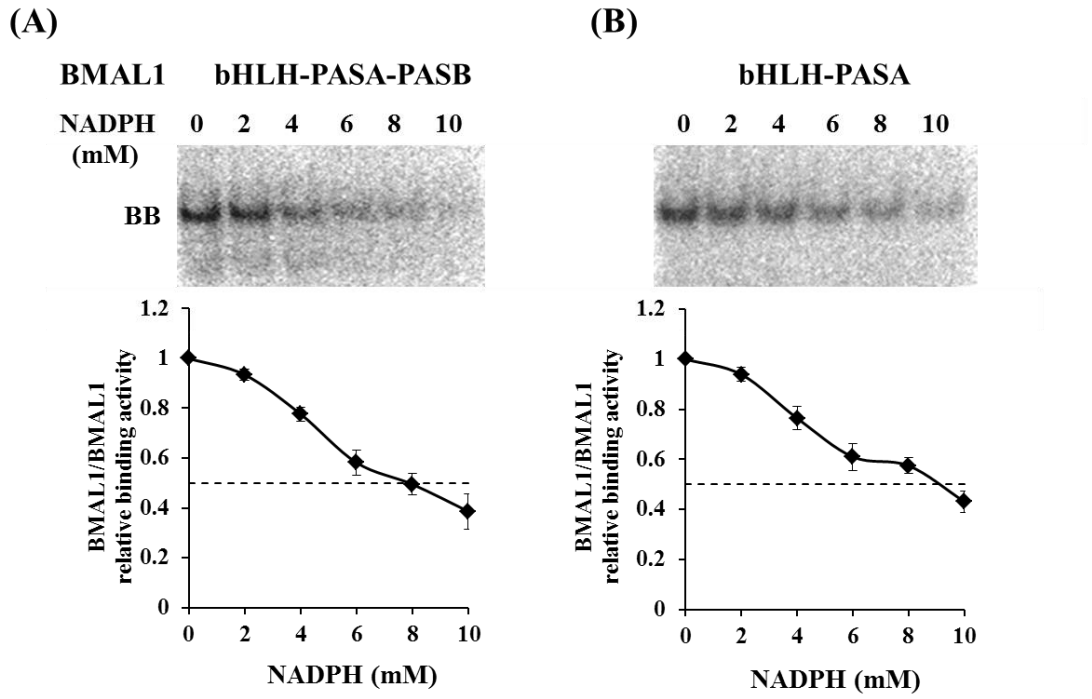

Figure 2-10. Effects of NADPH on the DNA-binding activity of MBP-BMAL1 bHLH-PASA-PASB (A) and MBP-BMAL1 bHLH-PASA (B) proteins. The DNA-binding activity of BMAL1 homodimer was quantified by Multi Gauge V2.1, and the activity represent a relative value normalized to the value obtained in the absence of NADPH. Each dot is the mean of at least three independent experiments ± SD.

2-3-4. Effects of NAD(P)H derivatives

To characterize the interaction between NPAS2 and NAD(P)H more precisely, the effects of various NAD(P)H derivatives on the DNA-binding activity of NPAS2/BMAL1 heterodimer were examined, and these compounds were also used to perform the competition assays with NAD(P)H. The derivatives used in this study were shown in Figure 2-11. Rutter *et al*. reported that $NADP^+$ inhibited the DNA-binding activity of NPAS2/BMAL1 heterodimer and competed with NADPH at an IC_{50} of 0.56 mM [51]. In their system, even addition of equimolar $NADP^+$ to a reaction mixture containing 2 mM NADPH completely inhibited the formation of the NPAS2/BMAL1/DNA complex. Unexpectedly, in the system of present study, $NADP^+$ itself had no effect on the DNA-binding activity of NPAS2/BMAL1 heterodimer (Figure 2-12A), and it did not compete with NADPH for the effect, even when the 5-fold excess of $NADP^+$ was added (Figure 2-12B). Similarly, NAD^+ neither affected the DNA-binding activity of NPAS2/BMAL1 heterodimer nor competed with NADH (Figure 2-13). The reasons for these inconsistencies are not clear, because the experimental conditions for EMS assay in this study are very similar to those described by Rutter *et al*. [51], except that they used the proteins purified from inclusion bodies, while proteins used in this study were purified from soluble fraction.

Other NADPH derivatives, namely 2',5'-ADP, nicotinamide, nicotinic acid and NAAD, were also examined for effects on the DNA-binding activity of NPAS2/BMAL1 heterodimer. As shown in Figure 2-14A, none of these compounds affected the DNA-binding activity of NPAS2/BMAL1 heterodimer when added individually. Furthermore, similarly to $NADP^+$, they did not either compete with NADPH by addition of 5-fold excess to it (Figure 2-14B). Similar results were obtained in competition assays using NPAS2 bHLH (1-61 a.a.). In all experiments, the pH values of NADPH derivative solutions were adjusted to 7.5 immediately before use, and it was carefully confirmed that the pH of the assay solution was not changed by the addition of excess derivatives during the assays, because some of them were highly acidic in aqueous solution. These results suggest that the reduced form of the nicotinamide moiety was critical for the effect of NAD(P)H. All of the reaction mixtures for EMS assays contained 2 mM DTT, suggesting that NAD(P)H might not work as a reducing agent

but rather that its structure was important for its effects.

NAD(P)H also enhanced the DNA-binding activity of CLOCK/BMAL1 heterodimer [51]. Recently, the crystal structures of the bHLH-PASA-PASB domains of murine CLOCK/BMAL1 heterodimer [53] and the bHLH domains of human CLOCK/BMAL1 heterodimer bound to E-box DNA have been reported [54]. As observed in other bHLH proteins, the N-terminal halves of the α1 helices of both CLOCK and BMAL1 contain many basic residues to bind DNA, and the C-terminal halves of the α1 helices form a four-helix bundle with the α2 helices to stabilize the CLOCK/BMAL1 heterodimer. Because the residues in the bHLH domain of CLOCK are highly conserved in the bHLH domain of NPAS2, the NPAS2/BMAL1 heterodimer is expected to bind to E-box DNA with a similar conformation. It is interesting to note that residues 1-61 of NPAS2 are sufficient to form the four-helix bundle of the heterodimer (Figure 2-9). Considering the structural requirements for DNA binding and heterodimer formation, the binding sites of NAD(P)H on NPAS2 may exist in the loop region. Further experiments are required to elucidate the molecular mechanism by which NADPH affects the DNA-binding activity of NPAS2/BMAL1 heterodimer or BMAL1 homodimer.

CLOCK is reported to be a histone acetyltransferase (HAT) whose activity is counterbalanced by SIRT1, an NAD^+-dependent histone deacetylase [17, 52]. The CLOCK/BMAL1 heterodimer activates transcription of *Nampt* which encodes a rate-limiting enzyme in the NAD^+ salvage pathway [18]. SIRT1 is recruited with the CLOCK/BMAL1 heterodimer and inhibits the transcription of *Nampt*. Thus, intracellular NAD^+ levels are regulated in a 24-hour cycle in a circadian manner; inversely, cell metabolism could regulate CLOCK function. Although NPAS2, unlike CLOCK, does not contain any regions with homology to HATs, another HAT, p300, exhibits a circadian time-dependent association with NPAS2 [56]. These results suggest that both CLOCK and NPAS2 could be regulated by cellular NAD^+/NADH levels via HAT-dependent chromatin remodeling. Therefore, the direct regulation of the DNA-binding activities of NPAS2 and CLOCK indicated in this chapter may act as an acute system that responds to fluctuations in intracellular NAD(P)H levels.

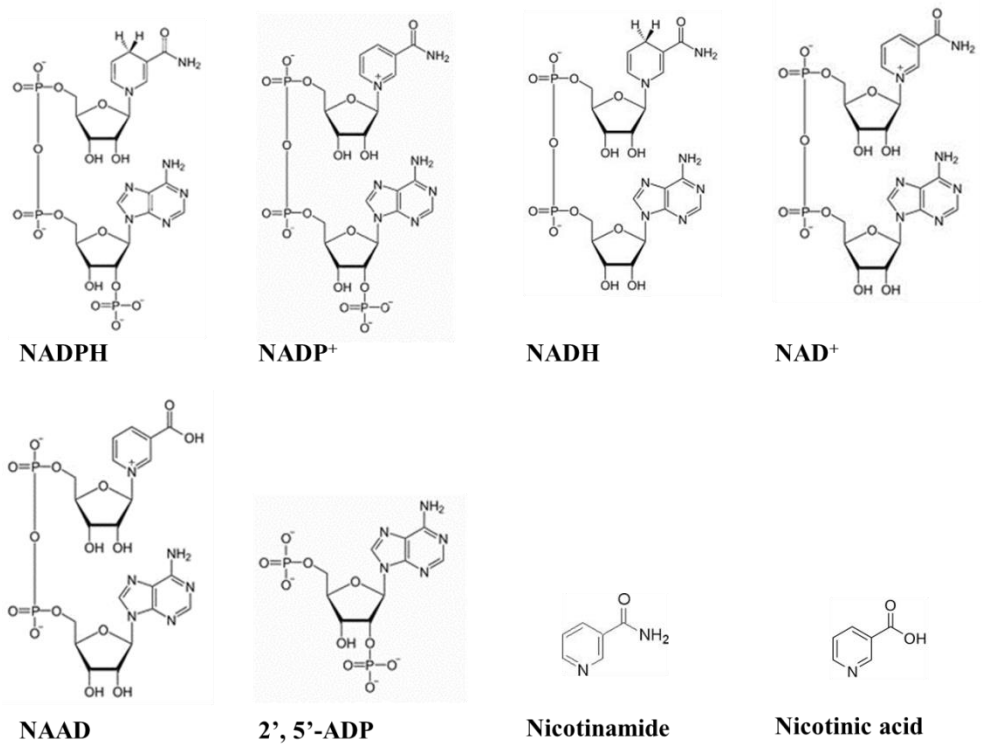

Figure 2-11. Structures of the NAD(P)H derivatives used in this study.

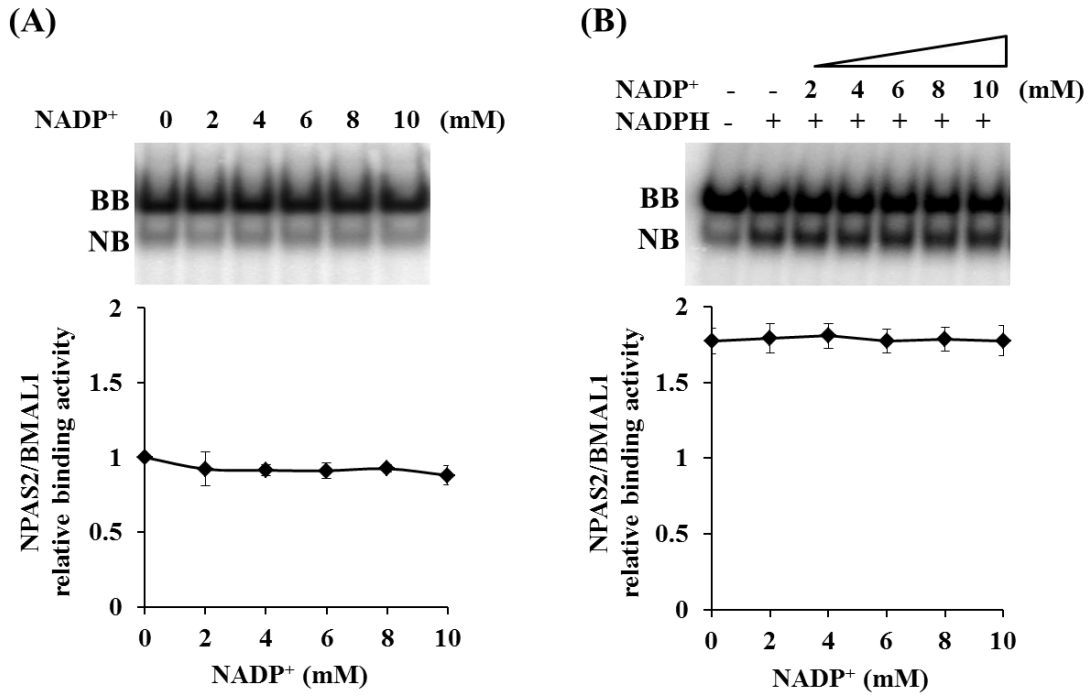

Figure 2-12. Effects of $NADP^+$ on the DNA-binding activity of NPAS2 bHLH-PASA and BMAL1 bHLH-PASA-PASB in the absence (A) or presence (B) of NADPH. The DNA-binding activity of NPAS2/BMAL1 heterodimer was not affected by addition of $NADP^+$ (A). $NADP^+$ did not compete with NADPH in the DNA-binding activity of the NPAS2/BMAL1 heterodimer (B). The independent experiments were conducted at least three times, and DNA-binding activity relative to that obtained without $NADP^+$ and NADPH is shown as the mean ± SD (n = 3).

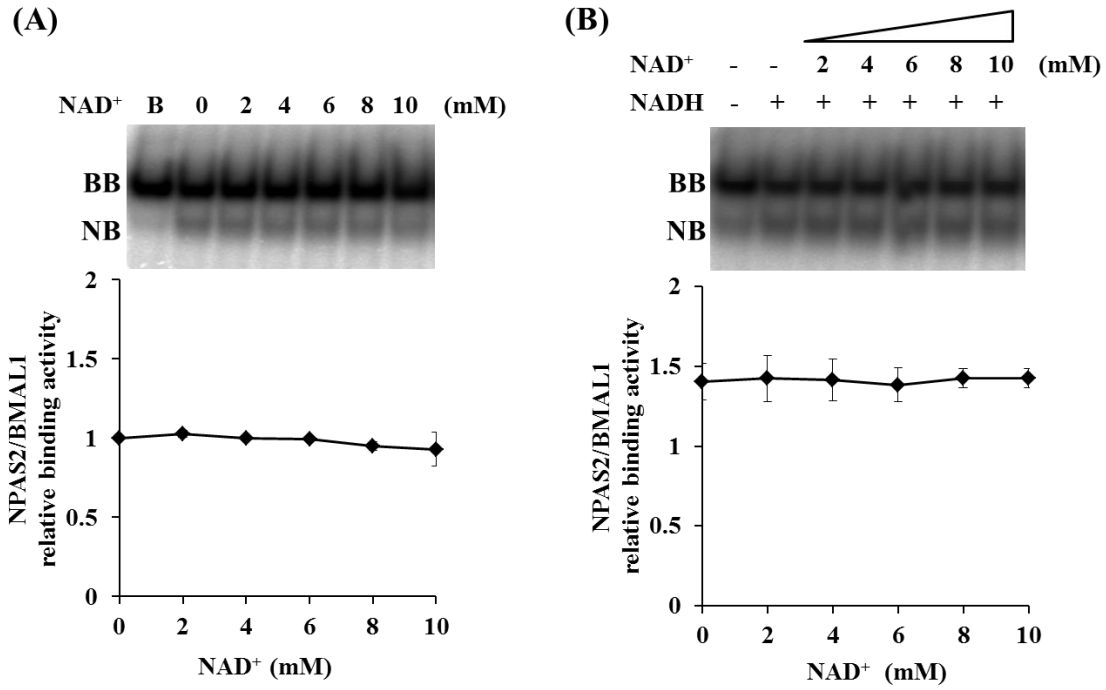

Figure 2-13. Effects of NAD^+ on the DNA-binding activity of NPAS2 bHLH-PASA and BMAL1 bHLH-PASA-PASB in the absence (A) or presence (B) of NADH. The DNA-binding activity of NPAS2/BMAL1 heterodimer was not affected by addition of NAD^+ (A). NAD^+ did not compete with NADH in the DNA-binding activity of the NPAS2/BMAL1 heterodimer (B). The independent experiments were conducted at least three times, and DNA-binding activity relative to that obtained without NAD^+ and NADH is shown as the mean ± SD (n = 3).

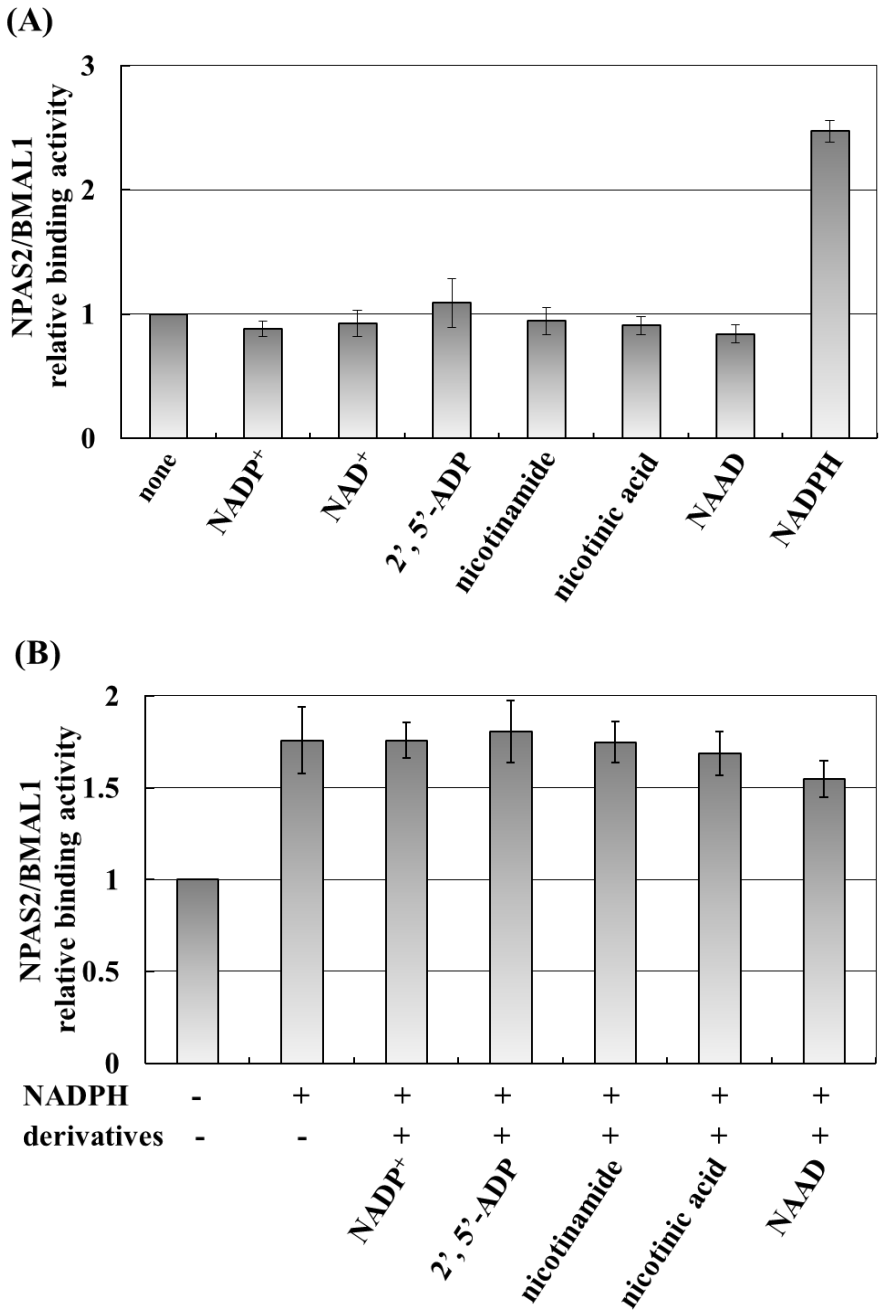

Figure 2-14. Effects of NAD(P)H derivatives on the DNA-binding activity of NPAS2 bHLH-PASA/BMAL1 bHLH-PASA-PASB heterodimer. Only NADPH had an effect; $NADP^+$, NAD^+, 2',5'-ADP, nicotinamide, nicotinic acid, and NAAD had no effect on the DNA-binding activity of NPAS2/BMAL1 heterodimer. All derivatives were examined at 10 mM (A). Competition assays with NAD(P)H derivatives in the presence of 2 mM NADPH. 10 mM of derivatives were added to the reaction mixture; other conditions are described in Materials and Methods (B).

Chapter 3.

pH and NAD(P)H additively regulate the DNA-binding activity of NPAS2

3-1. Introduction

In mammals, physiological and behavioral rhythms are controlled by the circadian molecular clock system [2-4]. The central clock, which exists in the hypothalamic suprachiasmatic nucleus (SCN), is entrained mainly by cycles of light and darkness, whereas the peripheral clocks in various tissues are synchronized by the central clock. At the molecular level, the circadian clock consists of transcriptional and translational feedback loops of clock genes and proteins [2-4].

Neuronal PAS domain protein 2 (NPAS2), a homolog of CLOCK, is a core transcription factor for mammalian circadian clock. Similar to CLOCK, NPAS2 forms a heterodimer with BMAL1, which binds to E-box or E-box-like elements in the regulatory regions of numerous clock genes and clock controlled genes to activate the expression of these genes [6, 32, 35]. NPAS2 consists of a bHLH domain, two PAS domains (PASA and PASB) and a transactivation domain. The bHLH domain of NPAS2 serves as a basic DNA-binding domain and a dimerization domain with other bHLH proteins. It was reported that the DNA-binding activity of the NPAS2/BMAL1 heterodimer was enhanced by NADH and NADPH [51]. Further, as described in the chapter 2, the bHLH domain of NPAS2 containing the N-terminal 1-61 amino acids was revealed to be sufficient to form a heterodimer with BMAL1, to bind to E-box and to sense NAD(P)H. The PAS domains of NPAS2, on the other hand, serve as protein-protein interaction sites for dimerization and heme-containing gas sensor domains [47, 48]. Although the two PAS domains bind heme, the main gas sensor is the PASA domain because the CO binding affinity of PASB-heme is less than 10% of that of PASA-heme [47]. The binding of CO to the heme of the PASA domain inhibits the DNA-binding activity of the NPAS2/BMAL1 heterodimer. During these studies, it was also found that the complex formation of the NPAS2/BMAL1 heterodimer with DNA was affected by pH.

Recently, two research groups reported that extracellular pH levels affected the expression rhythms of clock genes in cultured cells, indicating that pH could be a cue for the molecular clock [57, 58]. However, little is known about the molecular mechanism of the regulation of circadian rhythm by pH. Nonetheless, it is known that

pH plays a critical role in many cellular functions, such as the cell cycle, proliferation, metabolism, the synthesis of cellular macromolecules and signal transduction [59]. Therefore, the intracellular pH of mammalian cells is strictly maintained within a narrow range, even though it varies among different organelles. For example, the cytoplasmic and nuclear pH values are regulated at approximately 7.2, while those of mitochondria and lysosomes are approximately 8 and 4.7, respectively [60]. Additionally, the extracellular fluid has various pH values depending on the tissue and organ: the pH of plasma is slightly alkaline (7.3-7.4), while the digestive organs have a very low pH. Furthermore, extracellular acidification has been observed to be as low as pH 6.5 in tumor tissues in comparison to normal tissues [61]. In this chapter, therefore, the effects of pH on the DNA-binding activity of NPAS2 in vitro and NPAS2-dependent transcriptional activity in mammalian cells were examined. The additive effects of NADPH on the DNA-binding activity of NPAS2 were further elucidated under various pH conditions.

3-2. Materials and methods

3-2-1. Plasmid constructions

The expression plasmids for EMS assay, NPAS2 bHLH-PASA/pET-28a(+), NPAS2 bHLH/pET-28a(+) and BMAL1 bHLH-PASA-PASB/pMAL-c2X were described in the chapter 2-2-1. To create the expression plasmid for a truncation mutant of BMAL1, BMAL1 bHLH (74-128 a.a.), PCR was performed using pMAL-c2X containing BMAL1 bHLH-PASA-PASB cDNA as the template. The primers used for the PCR were 5'-GGGATCCCATATGAGGGAGGCCCACAGTC-3' as the sense primer and 5'-CGAATTCGTCGACTAGGCACCTCTCAAAG-3' as the antisense primer. The resulting product was subcloned into the *Nde* I and *Sal* I sites of pET-28a(+). The expression plasmid for His-tagged murine CLOCK bHLH-PASA (10-265 a.a.) was previously constructed [62]. The corresponding cDNA was cloned into the *Nde* I and *Sal* I sites of pET-28a(+). To create the expression plasmid for a truncation mutant of CLOCK, CLOCK bHLH (10-86 a.a.), PCR was performed using pET-28a(+) containing CLOCK bHLH-PASA (10-265 a.a.) cDNA as the template. The primers used for PCR were 5'-CGGGATCCCATATGAGCTCAATTG-3' as a sense primer and 5'-CCCGTCGACCTACTCTTTATGTTTGCGC-3' as antisense primer. The resulting product was subcloned into the *Nde* I and *Sal* I sites of pET-28a(+). All of the desired constructs were confirmed by sequencing.

The plasmids for a luciferase assay, *Npas2*/pCGN and *Bmal1*/pcDNA for expressing full-length murine NPAS2 (1-816 a.a.) and murine BMAL1 (1-626 a.a.), respectively, were previously constructed [52]. The corresponding cDNA of NPAS2 was cloned into the *Xba* I and *Hind* III sites of pCGN, and that of BMAL1 was cloned into the *Bam*H I and *Eco*R I sites of pcDNA. A reporter plasmid, m*Per1p*/pSLO, containing the murine *Per1* enhancer/promoter region (-1803 to +40) that has three canonical E-boxes (CACGTG) was also constructed previously by subcloning the region into the *Nhe* I and *Bgl* II sites of the pSLO-test vector [52]. Another reporter plasmid, m*Per1p*-E3M/pSLO was prepared by PCR-based method for mutation. In this reporter plasmid, all of the three E-boxes in m*Per1* enhancer/promoter region were mutated to TCTAGA. The desired mutations were confirmed by sequencing.

3-2-2. Expression and purification of truncated NPAS2, BMAL1 and CLOCK proteins

Expression and purification of the isolated bHLH-PASA (1-240 a.a.) or bHLH (1-61 a.a.) proteins of NPAS2 and the isolated bHLH-PASA-PASB (1-447 a.a.) protein of BMAL1 were carried out as described in the chapter 2-2-2 and 2-2-3, respectively, except that *E. coli* BL21-CodonPlus (DE3)-RIPL (Stratagene) was used as the host cell.

The His-tagged bHLH domain of BMAL1, BMAL1 bHLH (74-128 a.a.), was expressed in *E. coli* BL21-CodonPlus (DE3)-RIPL cells and purified similarly to His-NPAS2 bHLH. The purified protein was applied to a Sephadex G-25 column pre-equilibrated with buffer B to exchange the buffer to the appropriate one.

Expression of the isolated bHLH-PASA domains of CLOCK was performed using the plasmid CLOCK bHLH-PASA (10-265 a.a.)/pET-28a(+) with coexpression of *E. coli* chaperones, GroES and GroEL (the plasmid pGroESL was a gift from DuPont de Nemours and Co.), in BL21 (DE3) (Stratagene) cells. The cells were cultured and treated with 0.05 mM IPTG similarly to that of His-NPAS2 bHLH-PASA. The cell extract was prepared by sonication in buffer E (50 mM sodium phosphate, pH 7.8, 100 mM NaCl, 10% glycerol, 2 μg/ml aprotinin, 2 μg/ml leupeptin, 2 μg/ml pepstatin A, 1 mM PMSF, 0.2 mM DTT). After ultracentrifugation, the supernatant was adjusted to 50% saturated ammonium sulfate, incubated at 4 °C for 1 h and centrifuged again. The precipitate was dissolved in buffer E and applied to a Sephadex G-25 column pre-equilibrated with buffer E to remove ammonium sulfate. The resulting solution was applied to a Ni-NTA agarose column pre-equilibrated with buffer E and the column was sequentially washed with buffer E containing 50 mM and 80 mM imidazole. His-CLOCK bHLH-PASA was then eluted with buffer E containing 250 mM imidazole. The protein was applied to a Sephadex G-25 column pre-equilibrated with buffer B to remove the imidazole. His-CLOCK bHLH-PASA was prepared as holo-protein by reconstitution with hemin and apo-protein, similarly to His-NPAS2 bHLH-PASA.

Expression and purification of the isolated bHLH domain of CLOCK, CLOCK bHLH (10-86 a.a.), was carried out similarly to NPAS2 bHLH. The purified protein was applied to a Sephadex G-25 column to exchange the buffer with buffer B.

3-3-3. EMS assay

The ^{32}P-labeled E-box probe was prepared as described in the chapter 2-2-4 and purified with a gel-filtration column instead of ethanol precipitation. The concentration of labeled probe was determined in a competition analysis of the DNA-binding activity with unlabeled E-box probe whose concentration was spectrophotometrically estimated and confirmed on a 15% polyacrylamide gel by comparison with a double-strand DNA standard.

The DNA-binding reactions were typically performed as described in the chapter 2-2-4 in the presence or absence of 5 mM NADPH (Oriental yeast). To analyze the effects of pH on the DNA-binding activity of NPAS2/BMAL1 or CLOCK/BMAL1 heterodimer or BMAL1 homodimer, the pH of the reaction mixtures were varied from pH 6.5 to pH 8.5. In assays for the DNA-binding rate and affinity of the NPAS2/BMAL1 heterodimer or BMAL1 homodimer, the concentrations of proteins or DNA probe in the mixtures and the reaction time were variously altered for analysis, as described in detail in each figure legend.

The reaction mixtures were separated by electrophoresis on 5% or 7.5% (w/v) native acrylamide gels in buffer D for 2 h at 100 V and 4 °C. After electrophoresis, the gels were dried and analyzed as described in the chapter 2-2-4.

3-3-4. Cell culture and luciferase assay

NIH3T3 cells were seeded in 24-well plates (2×10^4 cells per well) (Iwaki) with DMEM (code no. 08456, Nacalai) containing 5% FBS (Equitech-bio) and cultured for 16 h at 37 °C under 5% CO_2 prior to transfection. The NPAS2 expression plasmid *Npas2*/pCGN (0.01 μg), the BMAL1 expression plasmid *Bmal1*/pcDNA (0.025 μg), a reporter plasmid, m*Per1p*/pSLO or m*Per1p*-E3M/pSLO (0.2 μg), and an internal control plasmid, pSLG-SV40 (0.025 μg) (Toyobo), were cotransfected into cells using Trans^{TM} First Reagent (Promega). The total amount of DNA was brought to 0.3 μg by the addition of the empty vector. After a 3-h treatment with the transfection mixture at 5% CO_2 and 37 °C, the medium was replaced with DMEM/5% FBS at pH 6.8, 7.2 or 7.7. Before use, the pH of the medium preincubated for 2 h at 37 °C and 5% CO_2 was adjusted and the medium was further incubated for 1 h at 37 °C and 5% CO_2; there was

little change in the pH of each medium (pH 6.8, 7.2 and 7.7, respectively) after another 24 h of cell culturing. The medium was then removed and the cells were lysed to analyze luciferase activities using MultiReporter Assay System-Tripluc^{TM}-Detection Reagents (Toyobo) according to the manufacturer's protocols. The relative luciferase activities were normalized to the activity obtained from the internal control, pSLG-SV40.

3-3. Results

3-3-1. DNA-binding activities of NPAS2 at various pH values in vitro

Several truncated proteins of NPAS2, BMAL1 and CLOCK were overexpressed and purified to examine the effects of pH on their DNA-binding activities. The domain structures of proteins used in this chapter are shown in Figure 3-1. All of the purified proteins were analyzed by SDS-PAGE, which showed more than 90% homogeneity (Figure 3-2). The UV-vis absorption spectra of the ferric, ferrous and CO-bound forms of His-NPAS2 bHLH-PASA and His-CLOCK bHLH-PASA were obtained as previously reported, confirming the structures of the PASA-domains [50].

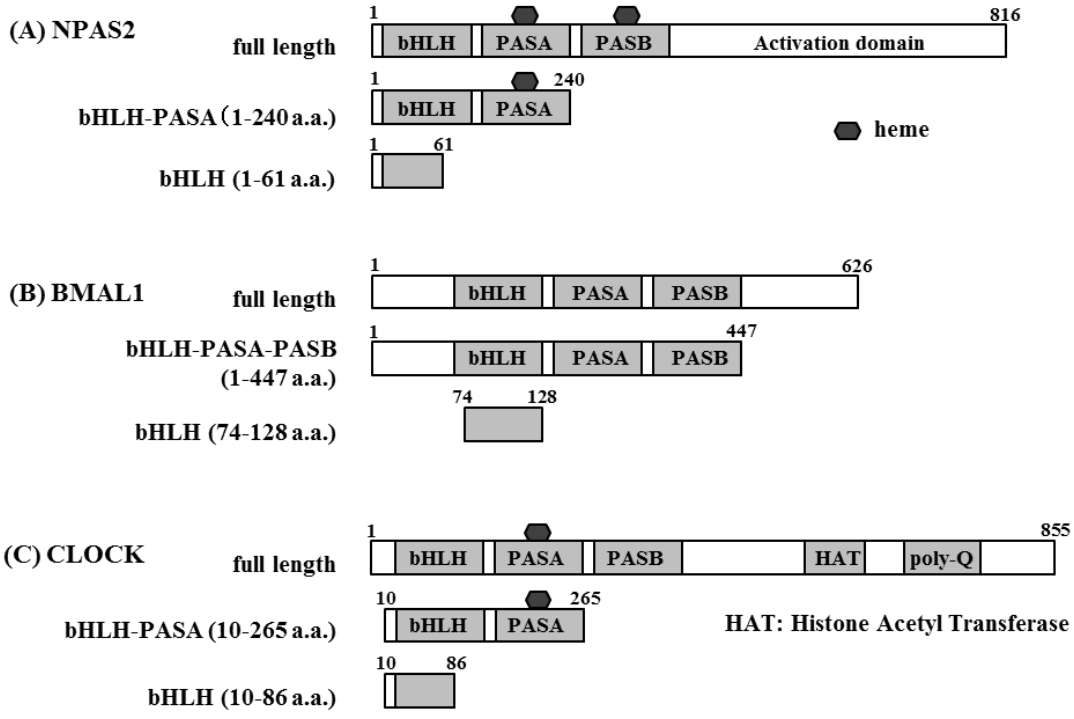

Figure 3-1. Domain structures of truncated NPAS2 (A), BMAL1 (B) and CLOCK (C) mutants used in this chapter.

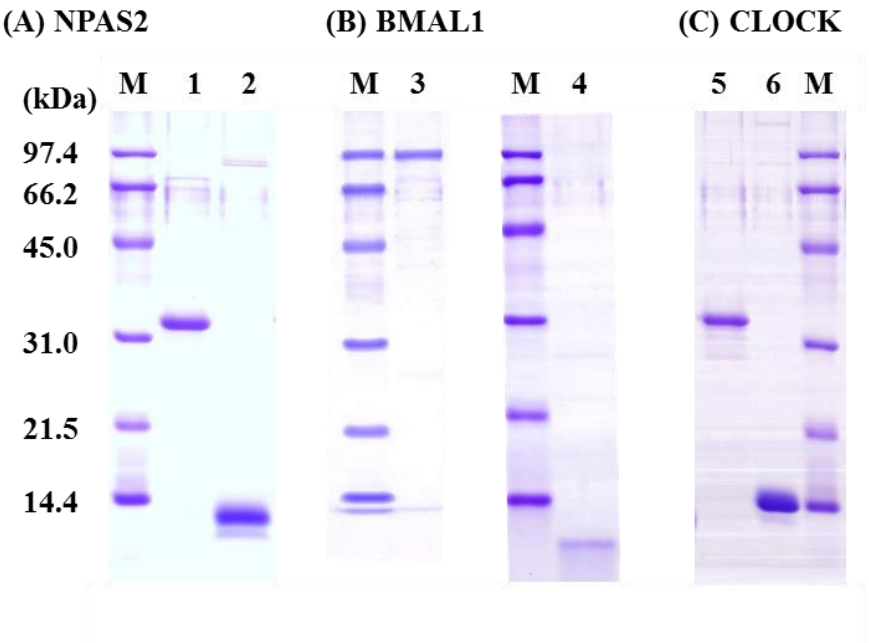

Figure 3-2. SDS-PAGE analyses of purified NPAS2 (A), BMAL1 (B), and CLOCK (C) mutants used in this chapter.
M; Molecular marker, 1; His-NPAS2 bHLH-PASA (1-240 a.a.),
2; NPAS2 bHLH (1-61 a.a.), 3; MBP-BMAL1 bHLH-PASA-PASB (1-447 a.a.),
4; BMAL1 bHLH (74-128 a.a.), 5; His-CLOCK bHLH-PASA (10-265 a.a.),
6; His-CLOCK bHLH (10-86 a.a.).

The DNA-binding activity of His-NPAS2 bHLH-PASA was examined at various pH values by an EMS assay. As shown in Figure 3-3A and 3-3B, the DNA-binding activity of the NPAS2/BMAL1 heterodimer increased with pH. Indeed, the activity at pH 8.5 was approximately 2.0- and 4.1-fold higher than that at pH 7.5 and pH 6.5, respectively, in the absence of NADPH. The addition of NADPH further increased the DNA-binding activity at each pH value. The DNA-binding activity increased up to 2.7-fold at pH 7.5 and 3.2-fold at pH 6.5 in the presence of NADPH (Figure 3-3B). These results indicate that the effects of pH and NADPH were additive in enhancing NPAS2/BMAL1/DNA complex formation. As described in the chapter 2-3-2, the N-terminal 61 amino acids of NPAS2, NPAS2 bHLH (1-61 a.a.), were sufficient to form a heterodimer with BMAL1, bind to the E-box and sense NADPH. Effects of pH on NPAS2 bHLH (1-61 a.a.) were also examined after the elimination of the His-tag by thrombin (Figure 3-3C). Similar to His-NPAS2 bHLH-PASA, the DNA-binding activity of NPAS2 bHLH was increased by pH and NADPH, indicating that the N-terminal 1-61 amino acids of NPAS2 were sufficient to sense pH and that these effects were independent of the His-tag (Figure 3-3C). Moreover, the DNA-binding activity of His-NPAS2 bHLH-PASA (1-240 a.a.) with BMAL1 bHLH (74-128 a.a.) without tag was also affected by pH, as with MBP-BMAL1 bHLH-PASA-PASB, indicating that the PASA and PASB domains of BMAL1 and MBP-tag were not responsible for the observed effects of pH alteration (Figure 3-4). The similar effects of pH and NADPH on the complex formation of the CLOCK/BMAL1 heterodimer with E-box DNA were observed, as shown in Figure 3-5. In the case of CLOCK, the bHLH domain containing 10-86 amino acids was essential and sufficient to sense pH and NADPH, similar to NPAS2.

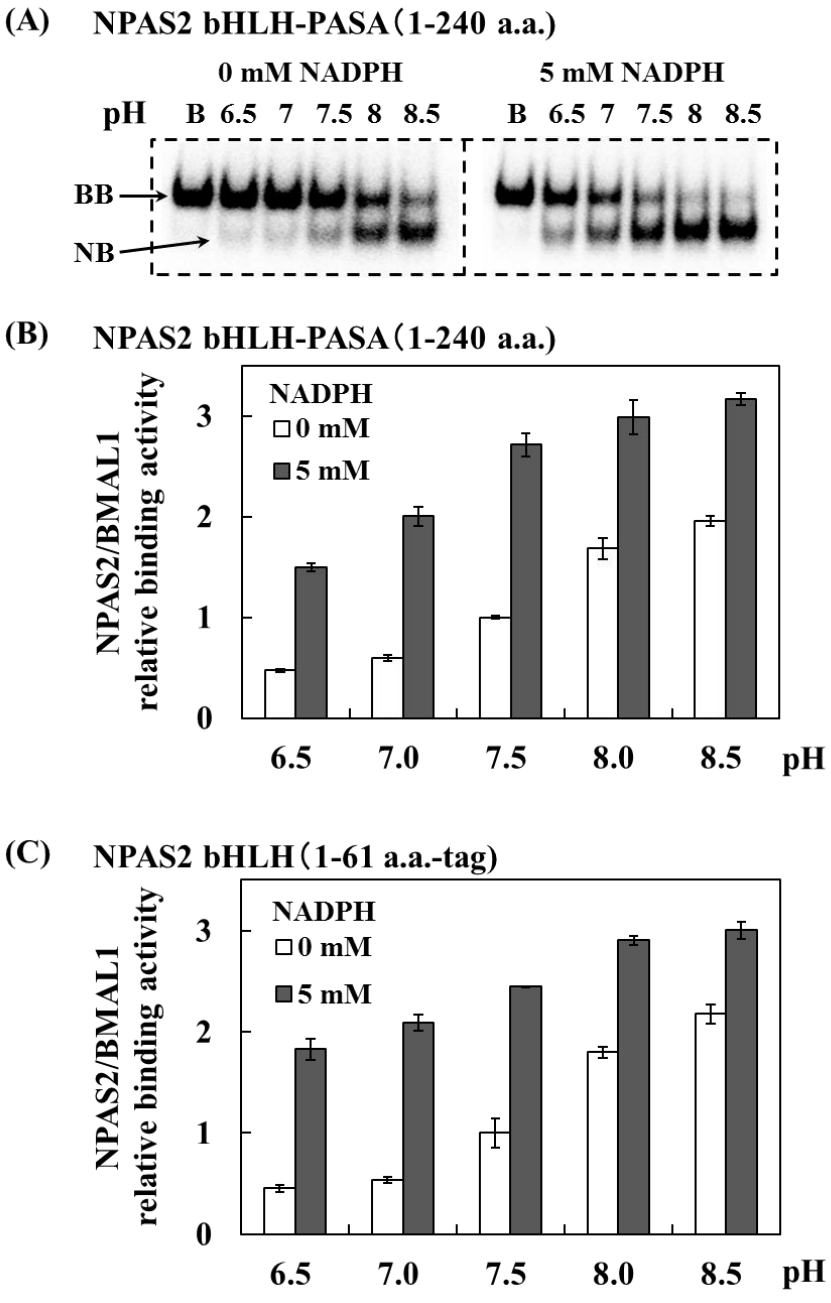

Figure 3-3. Effects of pH on the DNA-binding activity of NPAS2 bHLH-PASA (1-240 a.a.) and NPAS2 bHLH (1-61 a.a.). EMS assay using His-NPAS2 bHLH-PASA (1-240 a.a.) and MBP-BMAL1 bHLH-PASA-PASB at various pH values in the absence or presence of 5 mM NADPH. The label "B" at the top of the gel indicates an EMS assay in which the BMAL1 protein was incubated with DNA in the absence of NPAS2. BB, BMAL1/BMAL1 homodimer with ^{32}P-labeled E-box probe; NB, NPAS2/BMAL1 heterodimer with ^{32}P-labeled E-box probe (A). The relative DNA-binding activity of NPAS2/BMAL1 heterodimer at various pH in the absence (white) or presence (gray) of NADPH. The intensity of the bands shown in (A) was quantified by Multi Gauge V2.1 and represented as a relative value normalized to the value obtained at pH 7.5 in the

absence of NADPH. Each value is the mean of at least three independent experiments ± SD (B). The relative DNA-binding activity of His-NPAS2 bHLH (1-61 a.a.) with MBP-BMAL1 bHLH-PASA-PASB at various pH values in the absence or presence of 5 mM NADPH. The conditions for the EMS assay were the same as for (A), as described in "Experimental Procedures". Each value is the mean of at least three independent experiments ± SD (C).

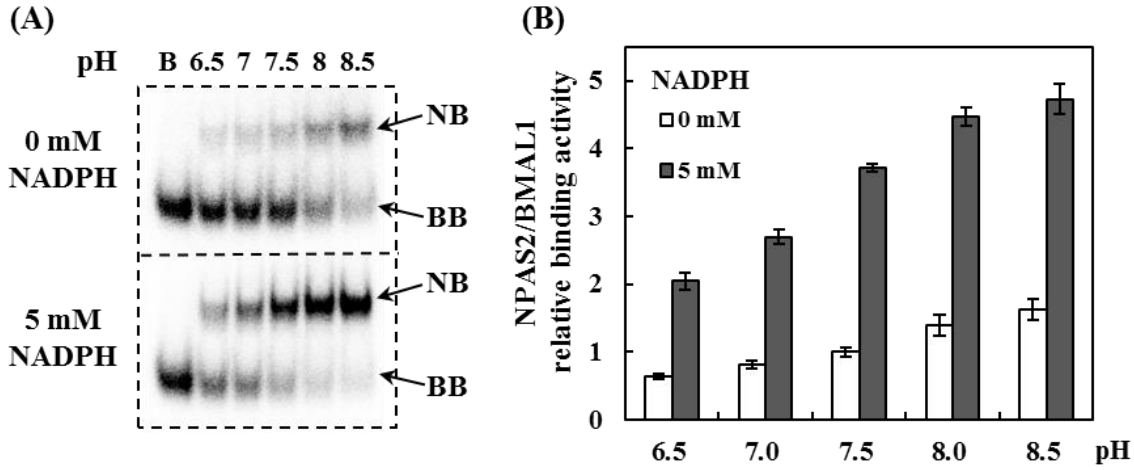

Figure 3-4. Effects of pH on the DNA-binding activity of His-NPAS2 bHLH-PASA (1-240 a.a.) and BMAL1 bHLH (74-128 a.a.) without tag. The EMS assay using His-NPAS2 bHLH-PASA and BMAL1 bHLH at various pH in the absence or presence of 5 mM NADPH. The label "B" at the top of the gel indicates an EMS assay in which BMAL1 protein was incubated with DNA in the absence of NPAS2. BB, BMAL1/BMAL1 homodimer with ^{32}P-labeled E-box probe; NB, NPAS2/BMAL1 heterodimer with ^{32}P-labeled E-box probe (A). The intensity of the bands shown in (A) was quantified by Multi Gauge V2.1 and represented as a relative value normalized to the value obtained at pH 7.5 in the absence of NADPH. Each value is the mean of at least three independent experiments ± SD (B).

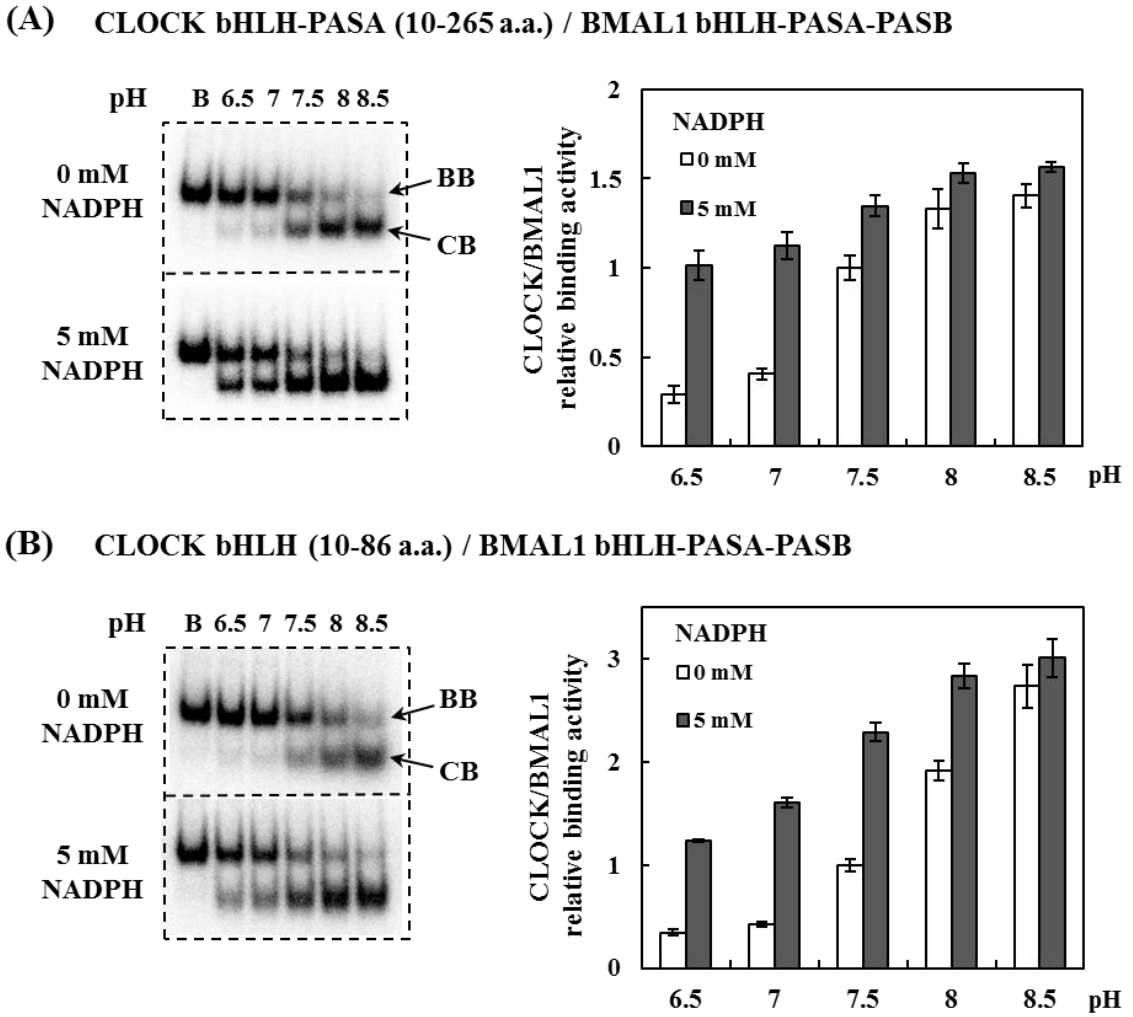

Figure 3-5. Effects of pH on the DNA-binding activity of His-CLOCK and MBP-BMAL1. The EMS assay using His-CLOCK bHLH-PASA (10-265 a.a.) (A) or His-CLOCK bHLH (10-86 a.a.) (B) and MBP-BMAL1 bHLH-PASA-PASB at various pH in the absence or presence of 5 mM NADPH. The label "B" at the top of the gel indicates an EMS assay in which BMAL1 protein was incubated with DNA in the absence of CLOCK. BB, BMAL1/BMAL1 homodimer with ^{32}P-labeled E-box probe; CB, CLOCK/BMAL1 heterodimer with ^{32}P-labeled E-box probe. The right panels indicate the relative DNA-binding activity of CLOCK/BMAL1 heterodimer at various pH in the absence (white) or presence (gray) of NADPH. The intensity of the bands was quantified by Multi Gauge V2.1 and represented as a relative value normalized to the value obtained at pH 7.5 in the absence of NADPH. Each value is the mean of at least three independent experiments ± SD.

3-3-2. DNA-binding activity of BMAL1 at various pH values

Since the DNA-binding activity of NPAS2/BMAL1 heterodimer was affected by pH, the effects of pH on the DNA-binding activity of BMAL1 homodimer was examined by an EMS assay in the absence of NPAS2. As shown in Figure 3-6, the DNA-binding activity of MBP-BMAL1 bHLH-PASA-PASB homodimer was not significantly affected by pH in the absence or presence of NADPH, though the addition of 5 mM NADPH rather inhibited the activity, as described in the chapter 2-3-3. These results indicate that NPAS2, but not BMAL1, is responsible for the regulation of the DNA-binding activity of NPAS2/BMAL1 heterodimer by pH. Therefore, further studies focused on the effects of pH and NADPH on the affinity of E-box DNA to NPAS2/BMAL1 heterodimer.

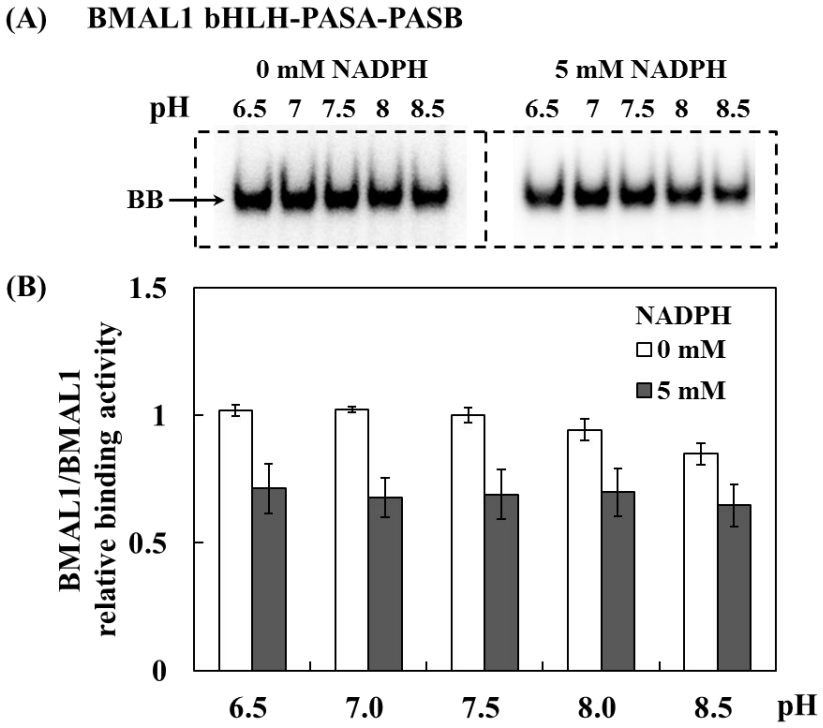

Figure 3-6. The DNA-binding activity of BMAL1 at various pH values in the absence of NPAS2. EMS assay using MBP-BMAL1 bHLH-PASA-PASB at various pH values in the absence or presence of NADPH (A). The DNA-binding activity of BMAL1/BMAL1 homodimer in the absence (white) or presence (gray) of NADPH. The intensity of the bands shown in (A) was quantified and represented as a relative value normalized to the value obtained at pH 7.5 in the absence of NADPH. Each value is the mean of at least three independent experiments ± SD (B).

3-3-3. Kinetics of DNA-binding of BMAL1 homodimer and NPAS2/BMAL1 heterodimer

To further elucidate the effects of pH and NADPH on the DNA-binding of the NPAS2/BMAL1 heterodimer, their kinetics were analyzed by an EMS assay with several modifications of the standard protocol, as described in the chapter 3-3-3. Initially, the DNA-binding rete of MBP-BMAL1 bHLH-PASA-PASB homodimer was examined at pH 7.5 in the absence of NPAS2. As shown in Figure 3-7, the DNA-binding activity of BMAL1 homodimer reached a plateau within 10 min in a reaction mixture containing 20 nM of BMAL1 as the monomer concentration and 50 nM of E-box DNA. Figure 3-8 shows the binding affinity of E-box DNA to BMAL1 homodimer, with an apparent dissociation constant (K_D^{app}) of 17 nM.

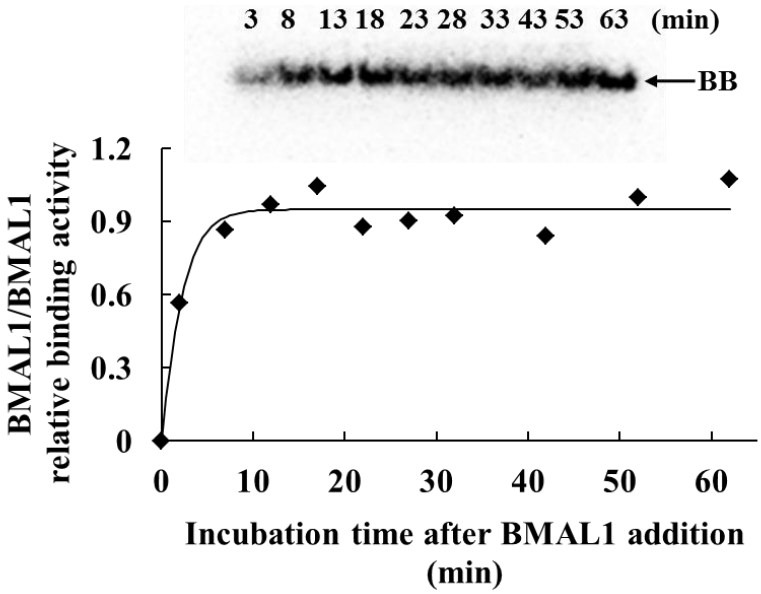

Figure 3-7. Time course of BMAL1 homodimer complex formation with DNA at pH 7.5 in EMS assay. The reaction mixture contained 20 nM MBP-BMAL1 bHLH-PASA-PASB and 50 nM E-box DNA (10 nM of ^{32}P-labeled and 40 nM of cold) in the absence of NPAS2, and was incubated on ice. The activity is represented as a relative value of BMAL/BMAL1 homodimer complex with DNA quantified by Multi Gauge V2.1.

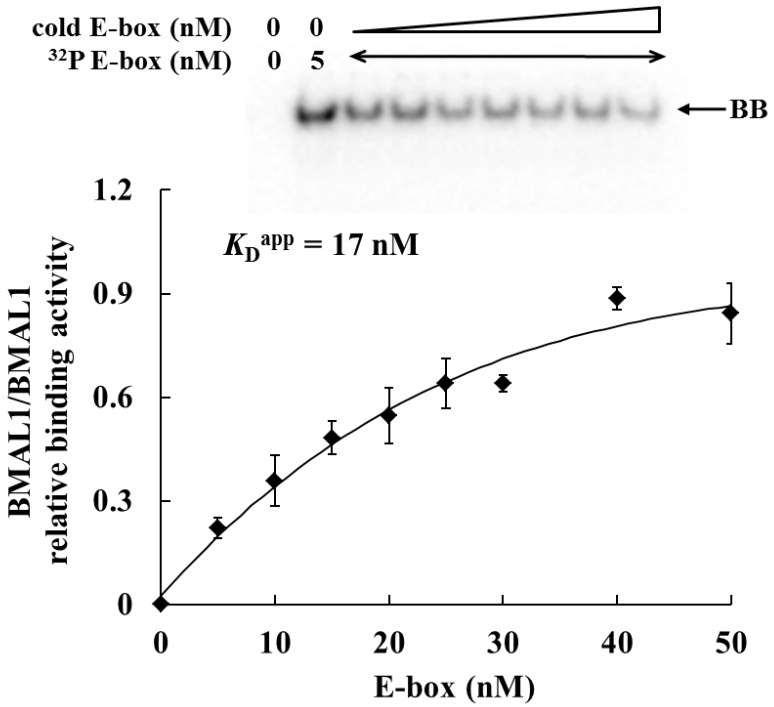

Figure 3-8. The effects of E-box DNA concentration on the complex formation of MBP-BMAL1 bHLH-PASA-PASB homodimer with DNA in EMS assay. The reaction mixtures contained 20 nM MBP-BMAL1 bHLH-PASA-PASB and various amount of E-box DNA, as indicated; incubation was for 30 min on ice. The activity is represented as a relative value of BMAL/BMAL1 homodimer complex with DNA quantified by Multi Gauge V2.1. Each value is the mean of at least three independent experiments ± SD.

After 20-min incubation for the equilibration between E-box DNA (50 nM) and BMAL1 (20 nM monomer), an excess amount of His-NPAS2 bHLH-PASA (400 nM) was added to the reaction mixture to examine the complex formation between NPAS2/BMAL1 heterodimer and E-box DNA. As shown in Figure 3-9, the dissociation of BMAL1 homodimer from E-box DNA was completed within 5 min and was immediately followed by the binding of NPAS2/BMAL1 heterodimer to E-box DNA in the absence of NADPH. The addition of NADPH to the system accelerated the dissociation of BMAL1 homodimer from E-box and the binding of NPAS2/BMAL1 heterodimer to E-box. It is noteworthy that the maximum amount of NPAS2/BMAL1/DNA complex was 0.6-fold of that of BMAL1/BMAL1/DNA complex in the absence of NADPH, demonstrating that the affinity of DNA to NPAS2/BMAL1 heterodimer was lower than that to BMAL1 homodimer under these conditions, consistent with the K_D^{app} values for NPAS2/BMAL1 heterodimer described below. In addition, the maximum amount of NPAS2/BMAL1/DNA complex was 3.7-fold that of BMAL1/BMAL1/DNA complex in the presence of NADPH, indicating that NADPH significantly increased NPAS2/BMAL1/DNA complex formation.

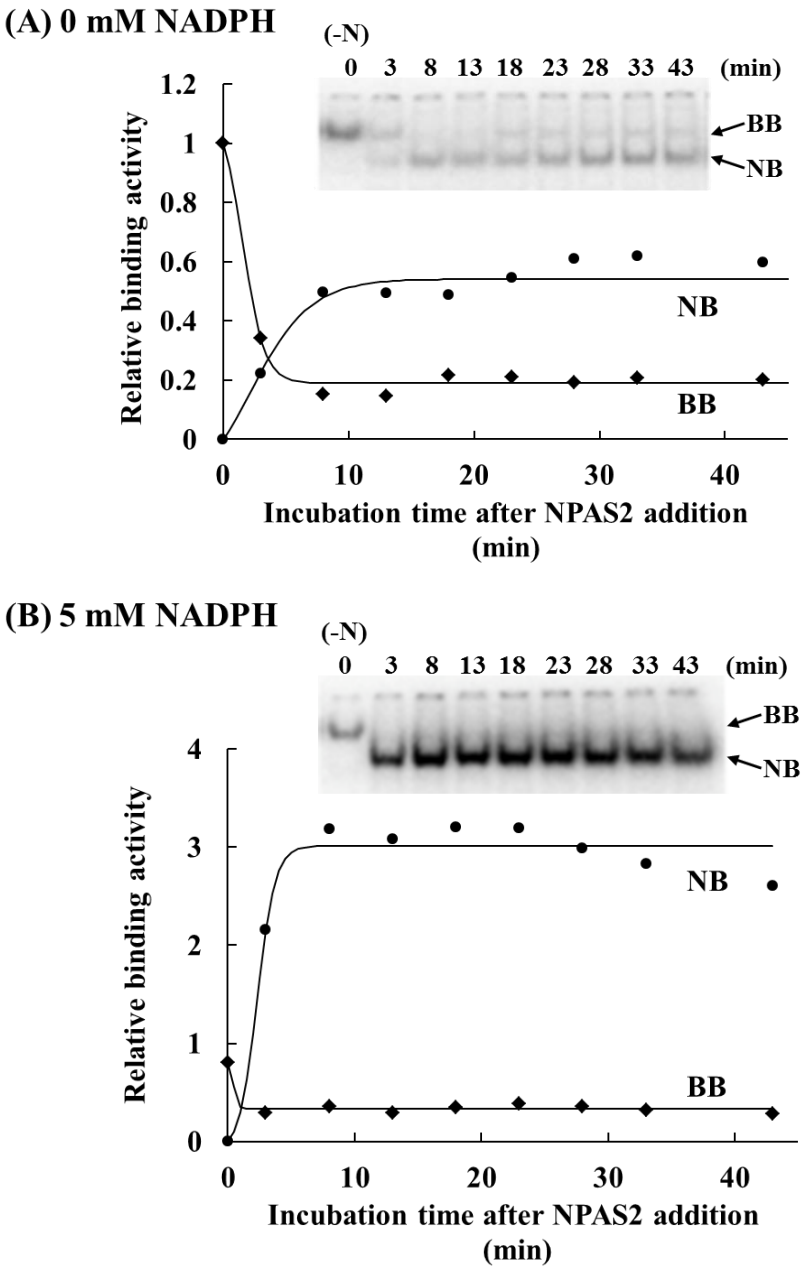

Figure 3-9. Time course of complex formation of NPAS2/BMAL1 heterodimer and decrease in BMAL1 homodimer complex with DNA at pH 7.5 in the absence (A) or presence (B) of NADPH in EMS assay. The reaction mixtures contained 50 nM E-box DNA, 20 nM MBP-BMAL1 bHLH-PASA-PASB and 400 nM of His-NPAS2 bHLH-PASA. After 20 min incubation on ice without NPAS2, NPAS2 was added to the reaction mixture and incubated on ice. The complexes with DNA were quantified by Multi Gauge V2.1 and represented as a relative value normalized to the value of the BMAL1 homodimer complex with DNA in the absence of NPAS2 and NADPH.

Next, the effects of the amount of NPAS2 relative to that of BMAL1 on the formation of the NPAS2/BMAL1/DNA complex were examined (Figure 3-10). Formation of the NPAS2/BMAL1/DNA complex was increased with an increasing concentration of NPAS2 in the reaction mixture, whereas formation of the BMAL1/BMAL1/DNA complex was decreased to an undetectable level in the EMS assay. In the absence of NADPH, the maximum DNA-binding activity of NPAS2/BMAL1 heterodimer was again lower than that of BMAL1 homodimer, even though the free probe was still abundant (more than 90% of the total amount) in the reaction mixture (Figure 3-10A). The addition of 5 mM NADPH resulted in great increase in NPAS2/BMAL1/DNA complex formation (Figure 3-10B). The amount of DNA used for both NPAS2/BMAL1/DNA and BMAL1/BMAL1/DNA complex formation was maximum 5% and 10% of the total amount in the absence and presence of NADPH, respectively, indicating that enough amount of free DNA still remained in the reaction mixture. These results also indicated that about 25% of BMAL1 protein was bound to the E-box DNA in the absence of NADPH. BMAL1 exists in equilibrium between BMAL1 dimer and oligomers in solution as shown in the results of gel-filtration (Figure 3-11), and the addition of DNA, NPAS2, and/or NADPH changes the equilibrium. In the presence of NADPH, the maximum amount of NPAS2/BMAL1/DNA increased to 2.7-fold of that of BMAL1/BMAL1/DNA (Figure 3-10B), indicating that more BMAL1 than that contained in BMAL1/BMAL1/DNA complex could form a heterodimer with NPAS2 and bound to DNA under conditions of the present study. A similar experiment was also performed at pH 7.0 (Figure 3-12). Although the shift in pH of the reaction mixture from pH 7.5 to pH 7.0 resulted in a decrease in the DNA-binding activity of NPAS2/BMAL1 heterodimer, NADPH again increased the formation of NPAS2/BMAL1/DNA complex. Taken together, these results demonstrated that 400 nM of NPAS2, which was 20-fold excess compared to BMAL1 (20 nM), was sufficient to saturate the formation of the NPAS2/BMAL1/DNA complex, with a background level of BMAL1/BMAL1/DNA complex formation.

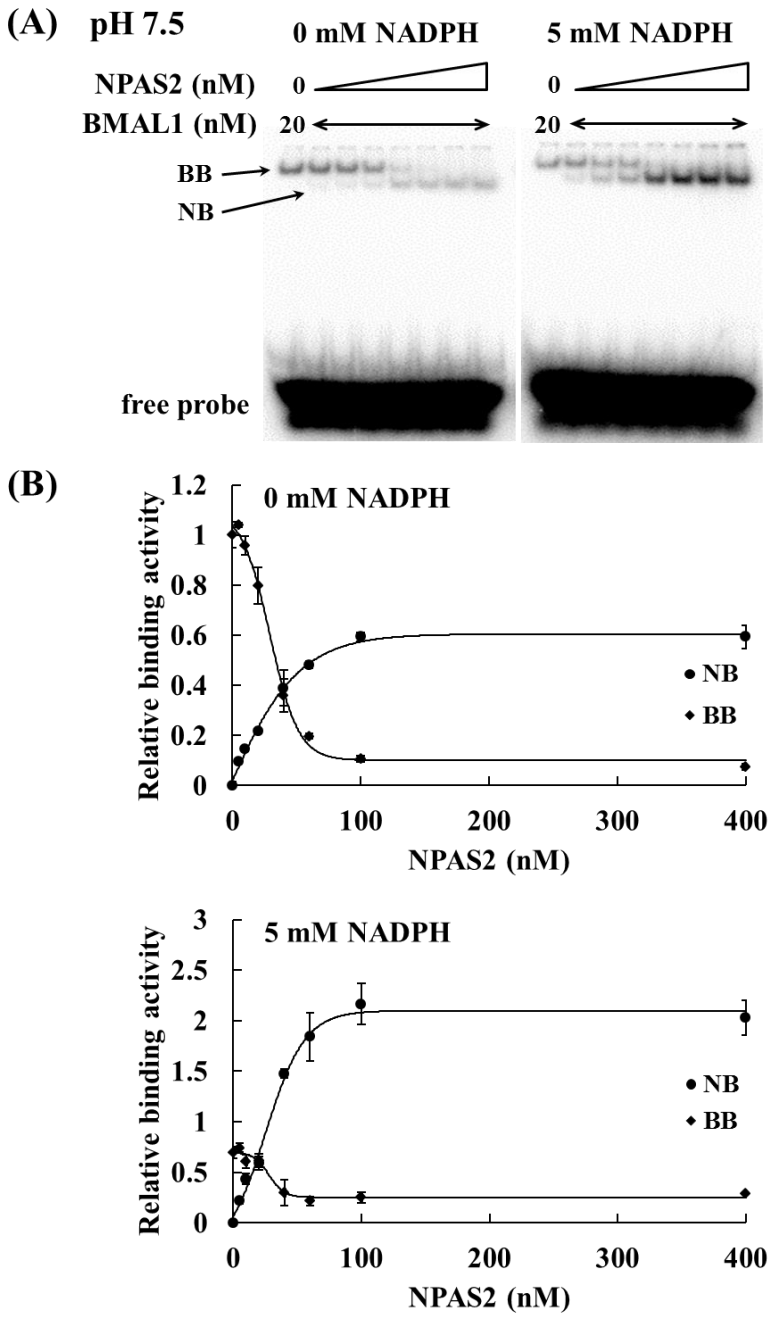

Figure 3-10. Effects of NPAS2 concentration on the complex formation of NPAS2/BMAL1 heterodimer with DNA. The reaction mixtures contained 50 nM E-box DNA, 20 nM MBP-BMAL1 bHLH-PASA-PASB and various concentrations of His-NPAS2 bHLH-PASA (0, 5, 10, 20, 40, 60, 100 and 400 nM) (A). The complexes with DNA in (A) were quantified by Multi Gauge V2.1 in the absence or presence of 5 mM NADPH and represented as a relative value normalized to the value of the BMAL1 homodimer complex with DNA in the absence of NPAS2 and NADPH (B).

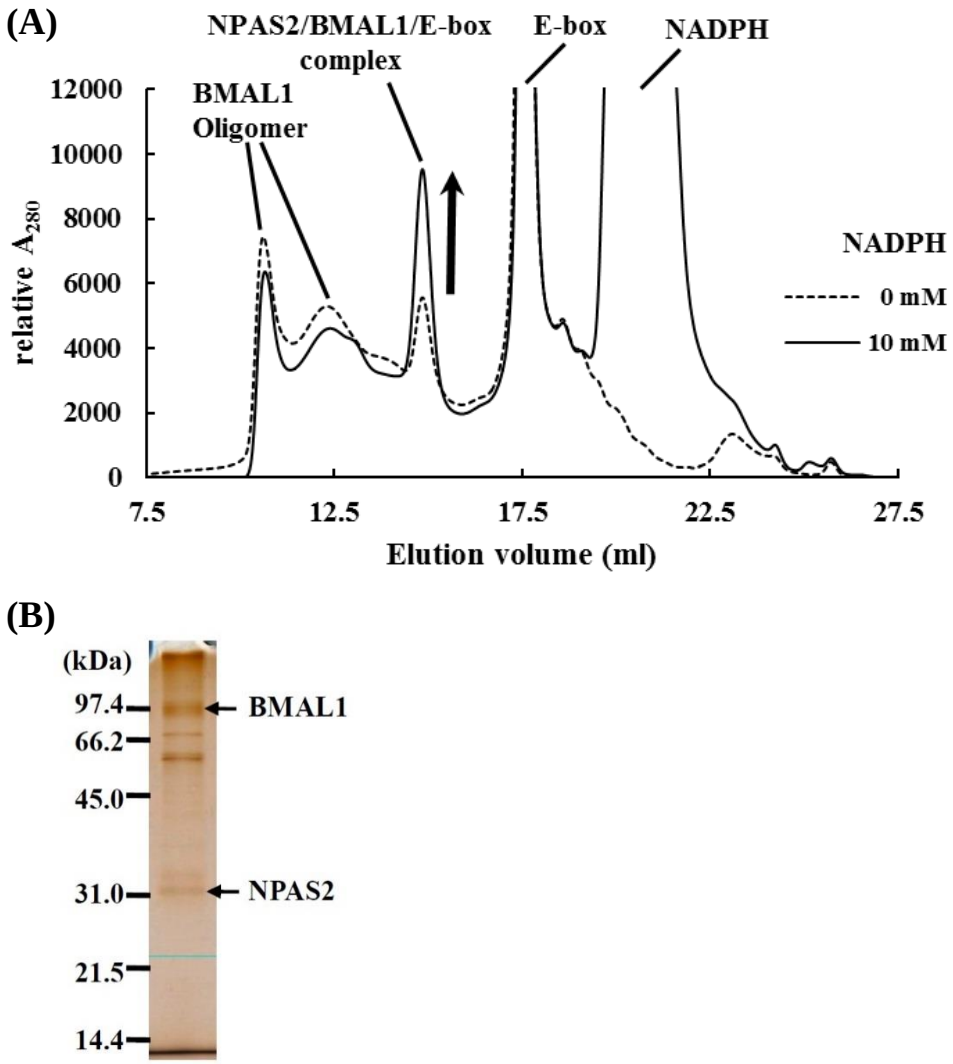

Figure 3-11. Gel filtration analysis of NPAS2/BMAL1/E-box complex. Elution profiles of NPAS2/BMAL1/E-box mixture. NPAS2 bHLH-PASA, BMAL1 bHLH-PASA-PASB and E-box (3 μM each) were incubated for 30 min in the absence (dashed line) or presence (solid line) of 10 mM NADPH on ice before the chromatography. The proteins, DNA, or NADPH were assigned to each peak based on the molecular weights estimated from the calibration curve obtained by using standard proteins (ferritin, BSA, OVA, myoglobin and RNase A). The peak(s) for NPAS2 bHLH-PASA was not detectable for the very low absorbance at 280 nm. column, COSMOSIL 5Diol-300-II; buffer, 100 mM Tris-HCl (pH 7.5), 10% glycerol, and 1 mM DTT; flow rate, 1 ml/min; temperature, r. t. (A). SDS-PAGE of the fraction eluted at around 15 ml from the gel-filtration column in the presence of NADPH with silver staining. The results confirmed that the fraction contained NPAS2 bHLH-PASA and BMAL1 bHLH-PASA-PASB (B).

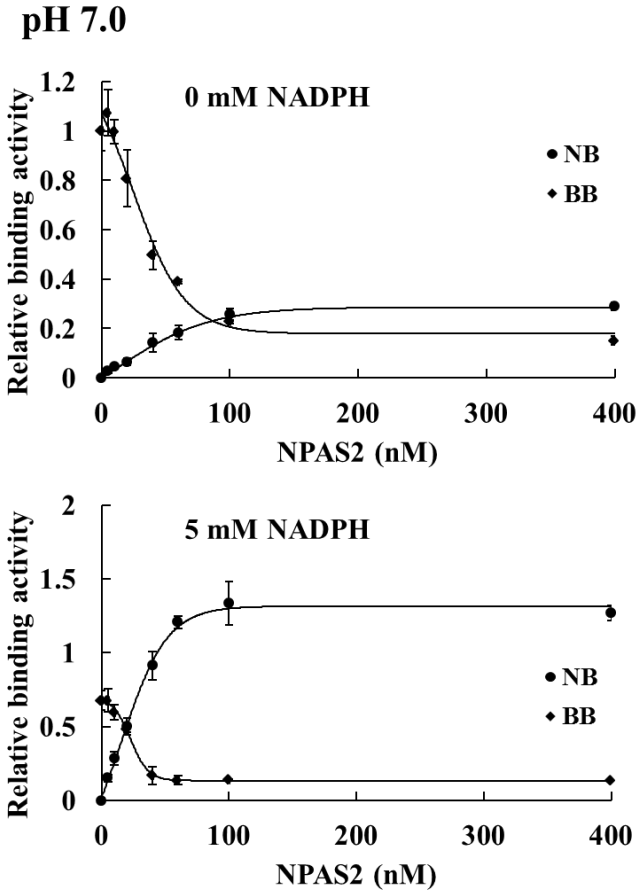

Figure 3-12. Effects of NPAS2 concentration on the complex formation of NPAS2/BMAL1 heterodimer with DNA at pH 7.0. Experimental procedures were described in Figure 3-10.

3-3-4. Effects of pH and NADPH on the DNA-binding affinity of NPAS2

To evaluate the effects of pH and NADPH on the DNA-binding activity of NPAS2 quantitatively, the apparent dissociation constant (K_D^{app}) of E-box DNA to the NPAS2/BMAL1 heterodimer was determined by EMS assay in a reaction mixture containing 400 nM of NPAS2 bHLH-PASA and 20 nM of BMAL1 bHLH-PASA-PASB with various concentrations of E-box DNA in the absence or presence of NADPH. High concentrations of E-box DNA were achieved by the addition of cold E-box DNA to the labeled probe. As expected, only bands corresponding to NPAS2/BMAL1 heterodimer were detected under these conditions (Figure 3-13A). The signals for the NPAS2/BMAL1/DNA complex were quantified and corrected to draw fitting curves (Figure 3-13B). At pH 7.5, the K_D^{app} values determined from the fitting curves were 45 and 14 nM in the absence and presence of NADPH, respectively. Similarly, the K_D^{app} values of the E-box DNA to NPAS2/BMAL1 heterodimer were determined at various pH conditions in the absence (Figure 3-14A) or presence of NADPH (Figure 3-14B), as summarized in Table 3-1. In the absence of NADPH, a pH change from 6.5 to 8.0 resulted in a decrease in the K_D^{app} value from 125 to 22 nM, with an 8-fold increase in the maximum level of DNA-binding of NPAS2/BMAL1 heterodimer (B_{max}). The K_D^{app} value was also decreased from 125 to 21 nM by the addition of NADPH at pH 6.5. In both the absence and presence of NADPH, the DNA-binding affinity of the NPAS2/BMAL1 heterodimer increased with pH, and it was further increased by the addition of NADPH, indicating that the effects of pH and NADPH were additive. Furthermore, the DNA-binding activity of NPAS2/BMAL1 heterodimer was more sensitive to pH in the absence of NADPH.

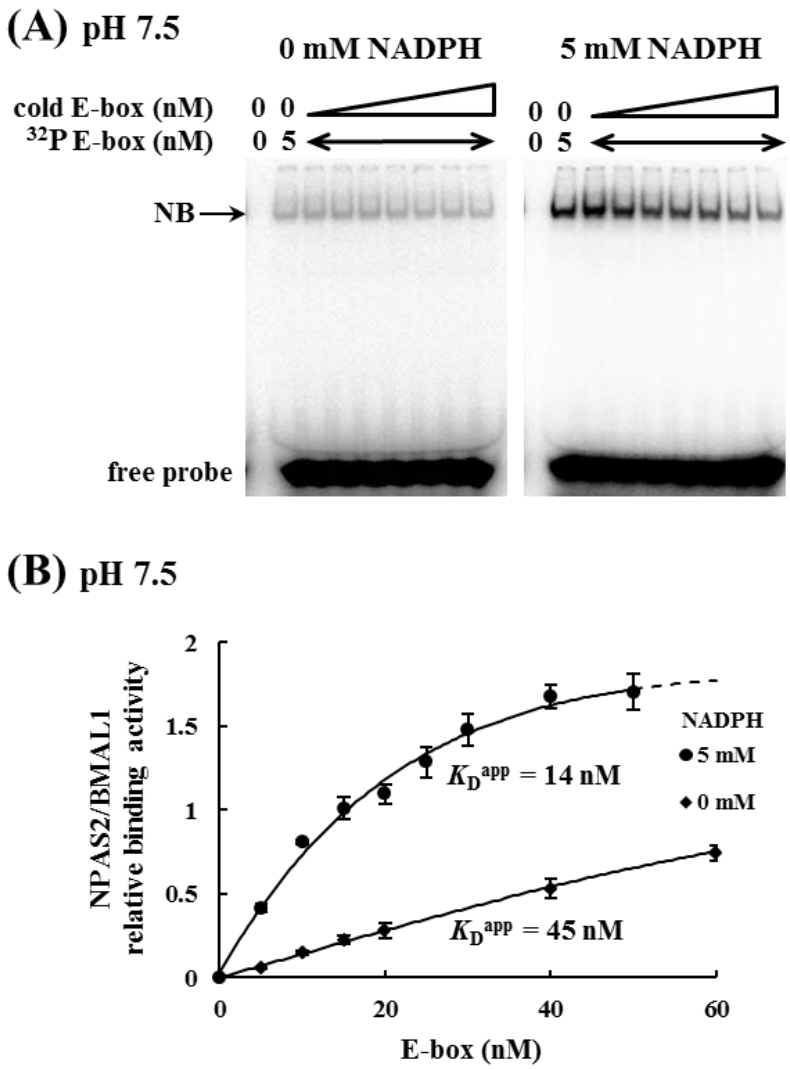

Figure 3-13. Effects of pH and NADPH on the DNA-binding affinity of NPAS2/BMAL1 heterodimer. EMS assays were performed with various amount of DNA at pH 7.5. The reaction mixtures contained 20 nM MBP-BMAL1 bHLH-PASA-PASB, 400 nM His-NPAS2 bHLH-PASA and various concentrations of E-box DNA (total 0, 5, 10, 15, 20, 40, 60, 80 and 100 nM of DNA in the absence of NADPH, or total 0, 5, 10, 15, 20, 25, 30, 40 and 50 nM of DNA in the presence of 5 mM NADPH). Each DNA contained 5 nM of ^{32}P-labeled probe (A). The DNA-binding activity of the NPAS2/BMAL1 heterodimer at pH 7.5 shown in (A) was quantified and represented as a relative value normalized to the maximum value obtained from the fitting curve in the absence of NADPH. Each dot is the mean of at least three independent experiments ± SD. The K_D^{app} values were estimated from a sigmoidal plot fitted to the data.

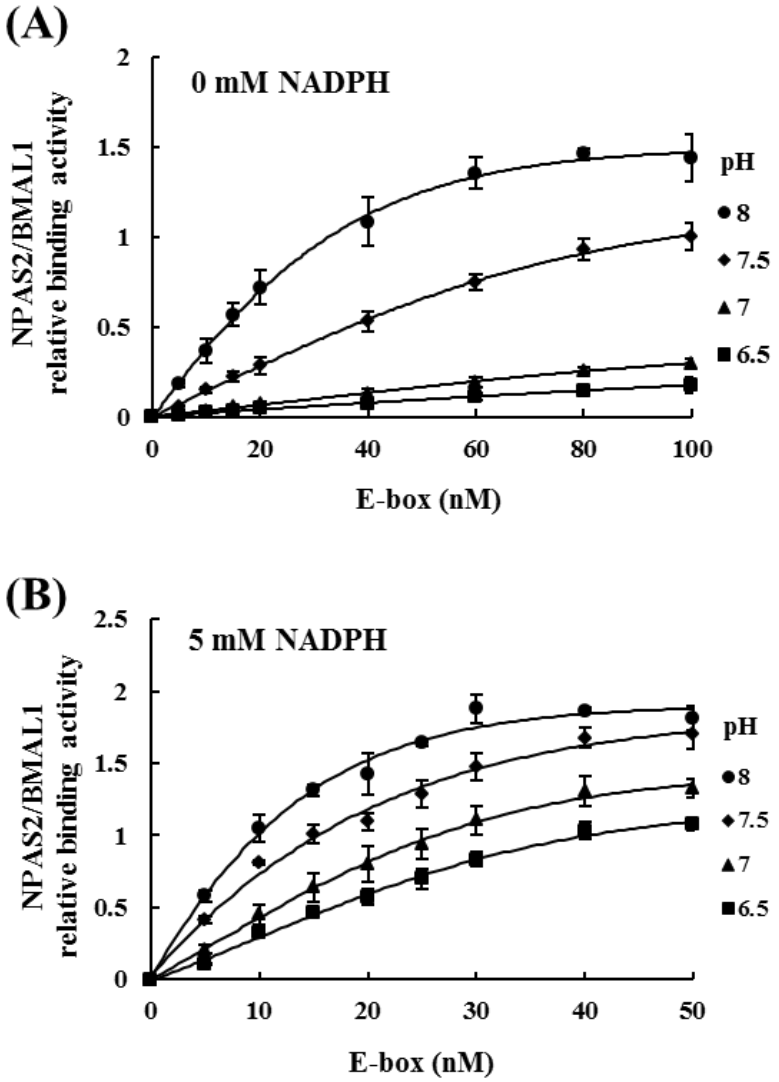

Figure 3-14. The DNA-binding affinity of NPAS2/BMAL1 heterodimer at various pH in the absence (A) or presence (B) of NADPH. All obtained data were analyzed as described for Figure 3-13. Each dot is the mean of at least three independent experiments ± SD. The K_D^{app} values estimated from a sigmoidal plot fitted to the data are summarized in Table 3-1.

Table 3-1. Effects of pH and NADPH on the K_D^{app} value of E-box DNA to the NPAS2/BMAL1 heterodimer and the maximum value of relative binding activity (B_{max}).

0 mM NADPH				
pH	6.5	7.0	7.5	8.0
K_D^{app} (nM)	125	61	45	22
B_{max}	0.18	0.29	1.00	1.44

5 mM NADPH				
pH	6.5	7.0	7.5	8.0
K_D^{app} (nM)	21	18	14	9
B_{max}	1.08	1.32	1.71	1.81

3-3-5. Effects of pH on the transcriptional activity of NPAS2 in cells

A luciferase assay in mouse NIH3T3 cells was carried out to investigate whether the transcriptional activity of NPAS2 was affected by extracellular pH. Two reporter plasmids, m*Per1p*/pSLO containing the enhancer/promoter region of mouse *Per1* (-1803 to +40) harboring three canonical E-boxes (CACGTG) and m*Per1p*-E3M/pSLO containing three-mutated E-boxes (M; TCTAGA) instead of canonical E-boxes in m*Per1* enhancer/promoter region, were used for assays (Figure 3-15A). The luciferase activities for both m*Per1p*/pSLO and m*Per1p*-E3M/pSLO without transfection of the NPAS2 expression plasmid did not change very much with increasing pH (6.8, 7.2 and 7.7). By the transfection of the full-length NPAS2 expression plasmid, the activities for m*Per1p*/pSLO significantly increased, whereas the activities for m*Per1p*-E3M/pSLO were not much affected (Figure 3-15B). The NPAS2-dependent transcriptional activity at each pH was evaluated by subtracting the activity without NPAS2 expression from that with NPAS2 expression. As shown in Figure 3-15C, the NPAS2-dependent transcriptional activity for m*Per1p*/pSLO increased with pH, whereas that for m*Per1p*-E3M/pSLO rather decreased. These results suggested that the extracellular pH affected the expression of the m*Per1* gene via E-box/NPAS2 in cells.

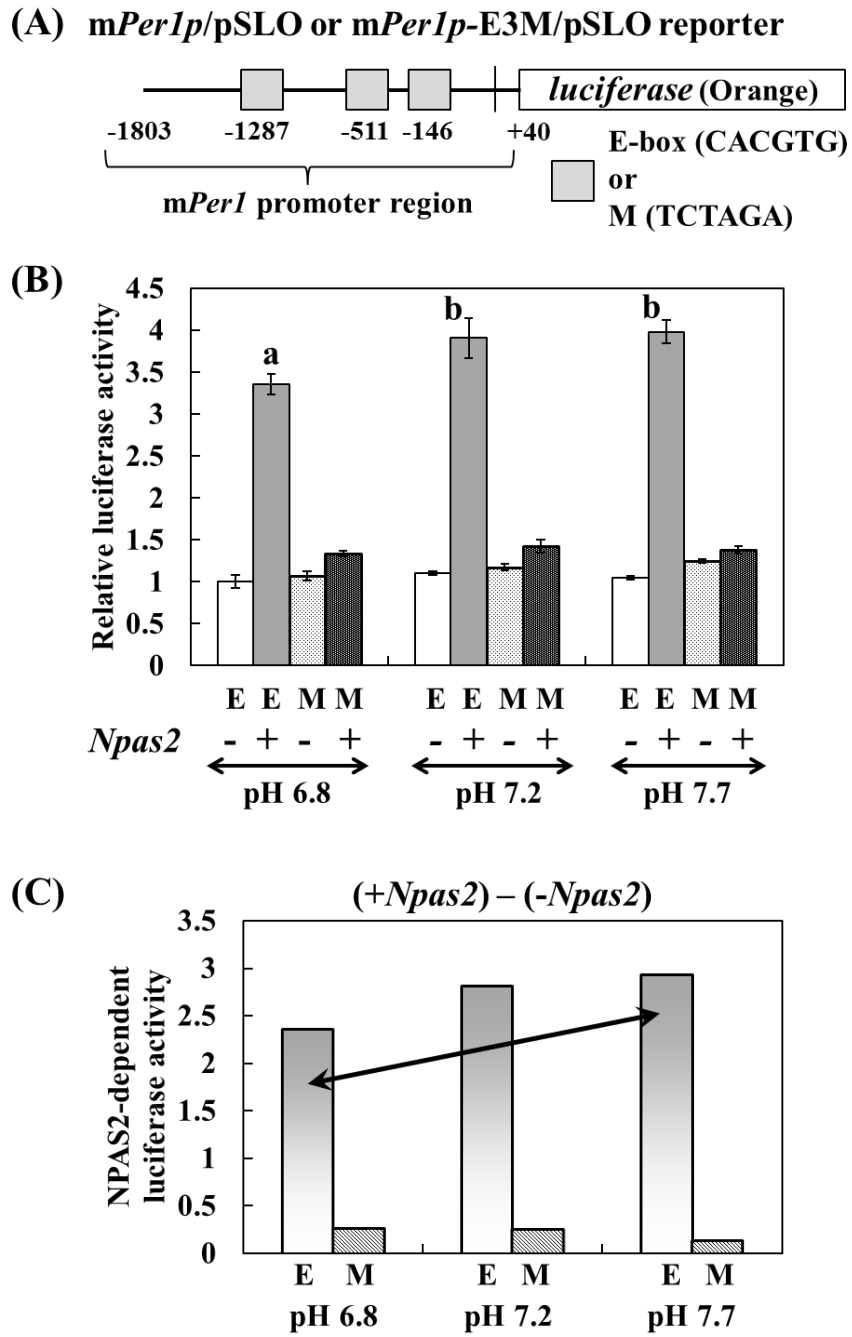

Figure 3-15. Effects of pH on the transcriptional activity of full-length NPAS2 in NIH3T3 cells. Construction of m*Per1p* and m*Per1p*-E3M reporter was illustrated. The m*Per1* promoter region contains three canonical E-boxes (CACGTG). In m*Per1p*-E3M reporter plasmid, all of the three E-boxes were mutated to TCTAGA (A). Relative luciferase activity for m*Per1p* (E) and m*Per1p*-E3M (M) reporter plasmids in cells cultured at pH 6.8, pH 7.2 and pH 7.7 for 24 h in the absence (-) or presence (+) of the NPAS2 expression plasmid, *Npas2*/pCGN. Luciferase activity is represented as a relative value to that obtained with m*Per1p* reporter and *Npas2* empty vector, pCGN, at pH 6.8. Each value is the mean of at least three independent experiments ± SD.

Significant differences between a and b were evaluated by the t test ($p < 0.02$) (B). NPAS2-dependent transcriptional activity via E-boxes increased with pH. The NPAS2-dependent luciferase activities for m*Per1p* (E) and m*Per1p*-E3M (M) reporter plasmids were calculated by subtracting the activities without *Npas2* from the activities with *Npas2* at each pH, as shown in (B) (C).

3-4. Discussion

In this chapter, using the EMS assay, it was showed that the DNA-binding activity of NPAS2/BMAL1 heterodimer increased with increasing pH. The addition of NADPH to the system further increased the complex formation of NPAS2/BMAL1 heterodimer with E-box DNA at each pH value, indicating that the observed pH and NADPH effects were additive (Figure 3-3). As described in the chapter 2-3-2, NADPH itself enhanced the DNA-binding activity of NPAS2/BMAL1 heterodimer. Conversely, the DNA-complex formation of BMAL1 homodimer, which is not functional as a transcription factor, was not affected by pH and NADPH (Figure 3-6). In addition, the N-terminal 1-61 amino acids of NPAS2, which are adequate for heterodimer formation with BMAL1 and binding to E-box DNA, were sufficient for the effects of pH on its DNA-binding activity. The bHLH domain (1-61 a.a.) of NPAS2 was also responsible for the NADPH effect, as reported in the chapter 2-3-2, suggesting that pH and NADPH were sensed by a similar region of NPAS2.

The K_D^{app} values of the E-box DNA to NPAS2-bHLH-PASA/BMAL1-bHLH-PASA-PASB heterodimer were obtained at various pH values in the presence or absence of NADPH (Table 3-1), and changes in pH and NADPH concertedly decreased the K_D^{app} value. Under experimental conditions in the present study, the K_D^{app} values were between 9-125 nM. These values for NPAS2/BMAL1 heterodimer were comparable to those for other bHLH-PAS family proteins, such as human HIF-1α/HIF-1β (ARNT) and mouse-DR/human-ARNT heterodimers [63]. Gel-filtration analysis suggested that in the system of present study, BMAL1 bHLH-PASA-PASB formed a higher-order oligomer than a dimer, and NPAS2 bHLH-PASA formed mainly dimers with a minor monomer fraction, indicating that all species of those existed in a dynamic equilibrium in solution. In the absence of NADPH, the mixture of NPAS2, BMAL1 and DNA revealed the partial formation of a heterodimer complex with DNA, and the addition of NADPH increased the formation of the heterodimer complex, with a decrease in BMAL1 oligomers (Figure 3-11). Therefore, under EMS conditions in the present study, it was postulated that formation of the complexes of DNA with BMAL1/BMAL1 homodimer and NPAS2/BMAL1

heterodimer were readily detectable though BMAL1 oligomer, NPAS2 oligomer, and NPAS2/NPAS2 homodimer did not form a detectable complex with DNA. Figure 3-9 demonstrated that the NPAS2/BMAL1/DNA complex was preferentially formed, with a decrease in the BMAL1/BMAL1/DNA complex, even though the K_D^{app} value of DNA to BMAL1 homodimer was smaller than that to NPAS2/BMAL1 heterodimer in the absence of NADPH and even in the presence of NADPH at a pH lower than 7.5. These results suggest that the formation of NPAS2/BMAL1 heterodimer was preferential to that of BMAL1 homodimer.

Recently, the K_D^{app} value of fluorescein-labeled E'-box DNA (CACGTT) to the murine CLOCK bHLH-PASA-PASB/BMAL1 bHLH-PASA-PASB heterodimer was reported to be 59 ± 7.3 nM by fluorescence anisotropy [53]. It was similar to the values of the NPAS2 bHLH-PASA/BMAL1 bHLH-PASA-PASB heterodimer obtained in this study, suggesting that the ability of the murine NPAS2/BMAL1 heterodimer to bind to the E-box DNA was comparable to the murine CLOCK/BMAL1 heterodimer. In contrast, the K_D value of E-box DNA to the human CLOCK bHLH/BMAL1 bHLH heterodimer was also reported to be 1.52 ± 0.10 μM by ITC measurement at pH 7.8 [54], which was 30 and 70 times larger than the values obtained in this study at pH 7.5 and 8.0, respectively (Table 3-1). These authors also reported that none of the NAD(P)H cofactors tested significantly affected the K_D value of the E-box DNA to the human CLOCK bHLH/BMAL1 bHLH heterodimer [54]. Although the reasons for these differences were not clear, each experiment used different protein expression systems and analysis methods. Because the PAS domain is known to play an important role in dimer formation for various PAS proteins, the PAS domains contained in NPAS2 and BMAL1 constructs used in this study to evaluate K_D^{app} values must have contributed to stabilizing NPAS2/BMAL1 heterodimer, resulting in an increase in its DNA-binding activity.

Interestingly, the effects of pH were observed only for the complex formation of NPAS2/BMAL1 or CLOCK/BMAL1 heterodimers with E-box DNA, but not for that of BMAL1 homodimer with E-box DNA. In addition, considering that the bHLH domain of NPAS2 and CLOCK is sufficient to sense pH, therefore, the differences among the bHLH domain of CLOCK, NPAS2 and BMAL1 should be focused on (Figure 3-16).

Two groups recently reported the crystal structures of the bHLH-PASA-PASB domains of the murine (m) CLOCK/BMAL1 heterodimer [53] and the bHLH domains of the human (h) CLOCK/BMAL1 heterodimer bound to E-box DNA [54]. Based on the structure, Wang *et al*. demonstrated that His84 of hCLOCK and Leu125 of hBMAL1 were critical residues involved in mutual recognition for heterodimer formation. His59, which is contained in construct of the bHLH domain of mNPAS2 (1-61 a.a.) as the only His, corresponds to His84 of hCLOCK. His has also been reported as a residue responsible for pH sensing among many pH sensor proteins, such as KcsA, ASIC1a and epithelial Na^+ channel [64-66]. Therefore, His59 of NPAS2 is a possible candidate for sensing pH and for the formation of a stable heterodimer with BMAL1. Ser38 and Ser42 of mCLOCK, corresponding to Ser13 and Ser17 of mNPAS2, respectively, were reported to reduce transcriptional activity in vivo when phosphorylated [22], but neither the S38E nor S42E mutation of hCLOCK had a significant influence on DNA binding in vitro [54]. At the interface between the bHLH domains of CLOCK (NPAS2) and BMAL1, Ser70 of hCLOCK (Thr46 of mNPAS2), which is not conserved in the bHLH domain of BMAL1, appears to interact with Lys87 of hBMAL1 and mBMAL1 (Figure 3-16). Ser70 also possibly affects heterodimer formation depending on pH. Further studies are required to elucidate the residues responsible for the effects of pH on NPAS2 and CLOCK.

In NIH3T3 cells, on the other hand, it was demonstrated that the NPAS2-dependent transcriptional activity of m*Per1* increased with extracellular pH (from pH 6.8 to pH 7.7), whereas that of reporter containing all mutated E-boxes rather decreased (Figure 3-15). These results suggest that the transcriptional activity depending E-box/NPAS2 is significantly affected by pH change even within the range of physiological pH, although it is not clear whether pH effect is direct, and if so, how extracellular pH affects the intracellular and nuclear pH under these conditions.

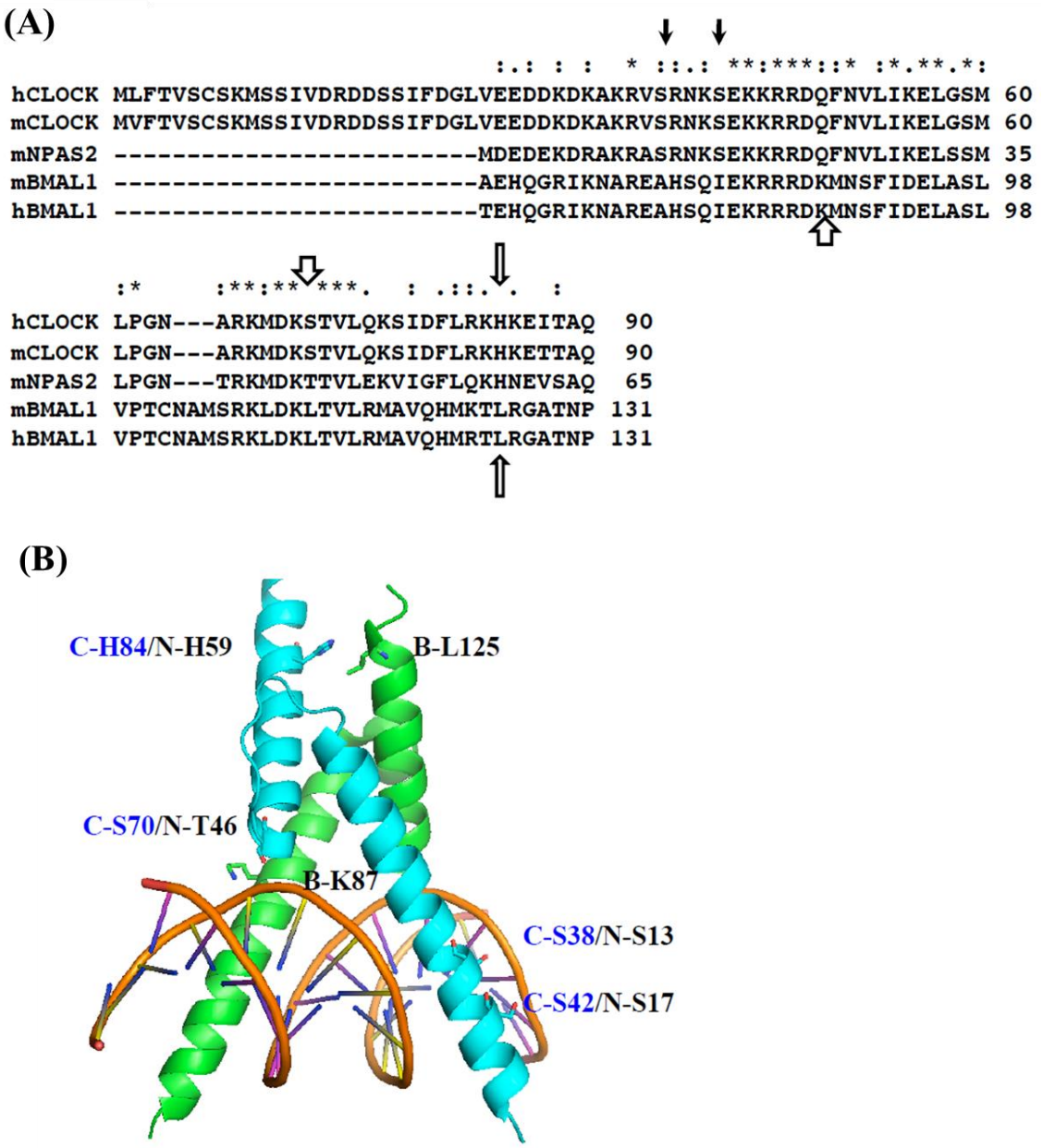

Figure 3-16. Multiple sequence alignment of the bHLH domains of human CLOCK, murine CLOCK, murine NPAS2, murine BMAL1, and human BMAL1. The arrows represent amino acid residues, Ser38, Ser42, Ser70 and His84 of hCLOCK, and Lys87 and Leu125 of hBMAL1 discussed in the text (A). Localization of the amino acids pointed in (A) in the structure of the bHLH DNA-binding domain of human CLOCK/BMAL1 heterodimer (PDB: 4H10) [54] (B).

Chapter 4.

Summary and conclusion

Molecular rhythms in mammalian cells and tissues can be entrained by various extra- and intracellular stimuli, such as light, temperature, hormone, gaseous signaling molecules and metabolites. These stimuli simultaneously and concertedly act on clock machinery to reset behavioral and physiological rhythms. In the present study, it was demonstrated that pH as well as NADPH had effects on the DNA-binding and transcriptional activity of NPAS2, a mammalian circadian transcription factor acting as a positive limb of core loops in the clock.

It has been suggested that the DNA-binding activity of NPAS2 is regulated by the intracellular redox state of NAD(P)H [51], although the mechanism remains unclear. In the chapter 2, EMS assays using several truncation mutants of the NPAS2 bHLH domain were performed to investigate the NAD(P)H interaction site of murine NPAS2. Among the mutants, NPAS2 containing the N-terminal 61 residues formed a heterodimer with BMAL1 to bind DNA, and NAD(P)H enhanced the binding activity, while NAD(P)H inhibited the DNA-binding activity of the BMAL1 homodimer in a dose-dependent manner. NAD(P)H derivatives such as 2', 5'-ADP, nicotinamide, nicotinic acid and nicotinic acid adenine dinucleotide (NAAD) did not affect the DNA-binding activity. Interestingly, $NAD(P)^+$, previously reported as an inhibitor, did not affect the DNA-binding activity of NPAS2 in the absence or presence of NAD(P)H in the system of present study. These results suggest that the DNA-binding activity of NPAS2 is specifically enhanced by NAD(P)H independently of $NAD(P)^+$ and that the N-terminal 1-61 amino acids of NPAS2 are sufficient to sense NAD(P)H.

On the other hand, it was reported that extracellular pH levels affect the expression rhythms of clock genes in cultured cells [57, 58]. In the chapter 3, therefore, the effects of pH on the DNA-binding activity of NPAS2 were investigated. In an EMS assay, the pH of the reaction mixture affected the DNA-binding activity of NPAS2/BMAL1 heterodimer but not that of BMAL1 homodimer. A change in pH from 7.0 to 7.5 resulted in a 1.7-fold increase in activity in the absence of NADPH, and NADPH additively enhanced the activity up to 2.7-fold at pH 7.5. The experiments using truncation mutants revealed that the N-terminal 1-61 amino acids of NPAS2 were sufficient to sense both the pH change and NADPH. The kinetics of the formation and DNA-binding of the NPAS2/BMAL1 heterodimer at various pH values were further

analyzed. In the absence of NADPH, a pH change from 6.5 to 8.0 decreased the K_D^{app} value of the E-box to NPAS2/BMAL1 heterodimer from 125 to 22 nM, with an 8-fold increase in the maximum level of DNA-binding of the heterodimer. The addition of NADPH resulted in a further decrease in K_D^{app} to 9 nM at pH 8.0. Taken together, both of NADPH and pH affects the equilibrium among BMAL1/BMAL1, NPAS2/NPAS2, NPAS2/BMAL1, and their complexes with the target DNAs as shown in Figure 4-1.

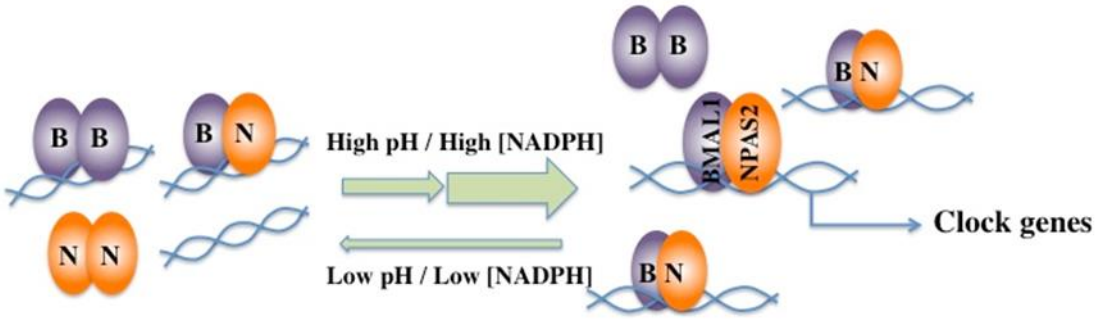

Figure 4-1. Schematic diagram to show the equilibrium among BMAL1/BMAL1, NPAS2/NPAS2, NPAS2/BMAL1, and their complexes with the target DNAs.

Furthermore, NPAS2-dependent transcriptional activity in a luciferase assay using NIH3T3 cells also increased with the pH of the culture medium. Although intracellular pH is generally strictly regulated within a narrow neutral region, it is known that the pH decreases in muscles after hard exercise due to the accumulation of pyruvate and lactate [67]. In cancer cells, extracellular acidification is caused by the enhancement of glycolysis that is sequentially followed by an increase in intracellular lactate and H^+, the induction of some of ion channels and receptors, and the efflux of these acids [61]. By means of the measuring autofluorescence lifetime of NADH, it was also demonstrated

that the alteration of cytosol pH induced pH change in nuclei in culture cells [68]. Interestingly, the results in the present study are consistent with the results of two other reports indicating the effects of extracellular pH on circadian rhythm [57, 58]. Kon *et al*. reported that alkali signals triggered a resetting of the molecular clock in cultured Rat-1 fibroblasts [57]. A pH shift in the culture medium in a range of 0.1–0.4 resulted in an increase in *Dec1* mRNA and consequently the phase-shift of the cellular rhythm. It was also reported that a pH change of the culture medium from 6.7 to 7.2 affected both the amplitude and the phase of the circadian expression of the hBMAL1 reporter in human primary fibroblasts [58]. In summary, the balance between NAD(P)H and pH appears to be a cue for the regulation of clocks via NPAS2 (CLOCK) under the various physiological conditions of tissues and cells, although further experiments are needed to elucidate precise mechanisms for sensing these signals.

Conclusions in the chapter 2.

1. NAD(P)H enhances the DNA-binding activity of NPAS2/BMAL1 heterodimer, but inhibits that of BMAL1/BMAL1 homodimer.
2. The N-terminal 1-61 amino acids of NPAS2 are sufficient to sense NAD(P)H.
3. $NAD(P)^+$, 2',5'-ADP, nicotinamide and NAAD do not affect the DNA-binding activity of NPAS2.

Conclusions in the chapter 3

1. The binding affinity of E-box to NPAS2/BMAL1 heterodimer increase with pH and additively by the presence of NADPH in vitro.
2. The N-terminal 1-61 amino acids of NPAS2 are sufficient to sense pH and NADPH.
3. NPAS2-dependent transcriptional activity regulating the m*Per1* gene also increase with extracellular pH in culture cells.

These results suggest that NPAS2 has a role as a pH and metabolite sensor to regulate circadian rhythms.

References

[1] Ebihara, S. and Yoshimura, T. (2012) Chronobiology. Kagakudojin. ISBN978-4-7598-1502-3.

[2] Ko, C. H., and Takahashi, J. S. (2006) Molecular components of the mammalian circadian clock. *Hum. Mol. Genet. 15,* 271-277.

[3] Liu, A. C., Lewis, W. G., and Kay, S. A. (2007) Mammalian circadian signaling networks and therapeutic targets. *Nat. Chem. Biol. 3,* 630-639.

[4] Buhr, E. D., and Takahashi, J. S. (2013) Molecular components of the mammalian circadian clock. *Handb. Exp. Pharmacol. 217,* 3-27.

[5] Gekakis, N., Staknis, D., Nguyen, H. B., Davis, F. C., Wilsbacher, L. D., King, D. P., Takahashi, J. S., and Weitz, C. J. (1998) Role of the CLOCK protein in the mammalian circadian mechanism. *Science 280,* 1564-1569.

[6] Kume, K., Zylka, M. J., Sriram, S., Shearman, L. P., Weaver, D. R., Jin, X., Maywood, E. S., Hastings, M. H., and Reppert, S. M. (1999) mCRY1 and mCRY2 are essential components of the negative limb of the circadian clock feedback loop. *Cell 98,* 193-205.

[7] Duong, H. A., Robles, M. S., Knutti, D., and Weitz, C. J. (2011) A molecular mechanism for circadian clock negative feedback. *Science 332,* 1436-1439.

[8] Preitner, N., Damiola, F., Molina, L. L., Zakany, J., Duboule, D., Albrecht, U., and Schibler, U. (2002) The orphan nuclear receptor REV-ERBα controls circadian transcription within the positive limb of the mammalian circadian oscillator. *Cell 110,* 251-260.

[9] Yin, L., and Lazar, M. A. (2005) The orphan nuclear receptor Rev-erbα recruits the N-CoR/histone deacetylase 3 corepressor to regulate the circadian *Bmal1* gene. *Mol. Endocrinol. 19,* 1452-1459.

[10] Solt, L. A., Kojetin, D. J., and Burris, T. P. (2011) The REV-ERBs and RORs: molecular links between circadian rhythms and lipid homeostasis. *Future Med. Chem. 3,* 623-638.

[11] Takeda, Y., Jothi, R., Birault, V., and Jetten, A. M. (2012) RORγ directly regulates the circadian expression of clock genes and downstream targets in vivo. *Nucleic Acids Res. 40,* 8519-8535.

[12] Ozaki, N., Noshiro, M., Kawamoto, T., Nakashima, A., Honda, K., Fukuzaki-Dohi, U., Honma, S., Fujimoto, K., Tanimoto, K., Tanne, K., and Kato, Y. (2012) Regulation of basic helix-loop-helix transcription factors *Dec1* and *Dec2* by RORα and their roles in adipogenesis. *Genes to Cells 17,* 109-121.

[13] Bass, J., and Takahashi, J. S. (2010) Circadian integration of metabolism and energetics. *Science 330,* 1349-1354.

[14] Oike, H., Nagai, K., Fukushima, T., Ishida, N., and Kobori, M. (2011) Feeding cues and injected nutrients induce acute expression of multiple clock genes in the mouse liver. *PLoS ONE 6,* e23709.

[15] Feng, D., and Lazar, M. A. (2012) Clocks, metabolism, and the epigenome. *Mol. Cell 47,* 158-167.

[16] Hirota, T., and Fukada, Y. (2004) Resetting mechanism of central and peripheral circadian clocks in mammals. *Zoolog. Sci. 21,* 359-368.

[17] Nakahata, Y., Sahar S., Astarita G., Kaluzova M. and Sassone-Corsi P. (2009) Circadian Control of the NAD^+ Salvage Pathway by CLOCK-SIRT1. *Science 324,* 654-657.

[18] Ramsey, K. M., Yoshino J., Brace C. S., Abrassart D., Kobayashi Y., Marcheva B., Hong H-K., Chong J. L., Buhr E. D., Lee C., Takahashi J. S., Imai S. and Bass J. (2009) Circadian Clock Feedback Cycle Through NAMPT-Mediated NAD^+ Biosynthesis. *Science 324,* 651-654.

[19] Rogers, P. M., Ying, L., and Burris, T. P. (2008) Relationship between circadian oscillations of Rev-erb expression and intracellular levels of its ligand, heme. *Biochem. Biophys. Res. Com. 368,* 955-958.

[20] Zhao, X., Cho, H., Yu, R. T., Atkins, A. R., Downes, M., and Evans, R. M. (2014) Nuclear receptors rock around the clock. *EMBO Rep. 15,* 518-528

[21] So, A. Y.-L., Bernal, T. U., Pillsbury, M. L., Yamamoto, K. R., and Feldman, B. J. (2009) Glucocorticoid regulation of the circadian clock modulates glucose homeostasis. *Proc. Natl. Acad. Sci. U. S. A. 106,* 17582-17587.

[22] Yoshitane, H., Takao, T., Satomi, Y., Du, N. H., Okano, T., and Fukada, Y. (2009) Roles of CLOCK phosphorylation in suppression of E-box dependent transcription. *Mol. Cell. Biol. 29,* 3675-3686.

[23] Um, J. H., Pendergast, J. S., Springer, D. A., Foretz, M., Viollet, B., Brown, A., Kim, M. K., Yamazaki, S., and Chung, J. H. (2011) AMPK regulates circadian rhythms in a tissue- and isoform-specific manner. *PLoS ONE 6,* e18450.

[24] Cardone, L., Hirayama, J., Giordano, F., Tamaru, T., Palvimo, J. J., and Sassone-Corsi, P. (2005) Circadian clock control by SUMOylation of BMAL1. *Science 309,* 1390-1394.

[25] Shirogane, T., Jin, J., Ang, X. L., and Harper, J. W. (2005) SCFβ-TRCP controls clock-dependent transcription via casein kinase 1-dependent degradation of the mammalian period-1 (Per1) protein. *J. Biol. Chem. 280,* 26863-26872.

[26] Yoo, S. H., Mohawk, J. A., Siepka, S. M., Shan, Y., Huh, S. K., Hong, H. K., Kornblum, I., Kumar, V., Koike, N., Xu, M., Nussbaum, J., Liu, X., Chen, Z., Chen, Z. J., Green, C. B., and Takahashi, J. S. (2013) Competing E3 ubiquitin ligases govern circadian periodicity by degradation of CRY in nucleus and cytoplasm. *Cell 152,* 1091-1105.

[27] Hirano, A., Yumimoto, K., Tsunematsu, R., Matsumoto, M., Oyama, M., Kozuka-Hata, H., Nakagawa, T., Lanjakornsiripan, D., Nakayama, K. I., and Fukada, Y. (2013) FBXL21 regulates oscillation of the circadian clock through ubiquitination and stabilization of cryptochromes. *Cell 152,* 1106-1118.

[28] Lamia, K. A., Sachdeva, U. M., DiTacchio, L., Williams, E. C., Alvarez, J. G., Egan, D. F., Vasquez, D. S., Juguilon, H., Panda, S., Shaw, R. J., Thompson, C. B., and Evans, R. M. (2009) AMPK regulates the circadian clock by cryptochrome phosphorylation and degradation. *Science 326,* 437-440.

[29] Busino, L., Bassermann, F., Maiolica, A., Lee, C., Nolan, P. M., Godinho, S. I., Draetta, G. F., and Pagano, M. (2007) SCFFbxl3 controls the oscillation of the circadian clock by directing the degradation of cryptochrome proteins. *Science 316,* 900-904.

[30] Ukai, H., and Ueda, H. R. (2010) Systems biology of mammalian circadian clocks. *Annu. Rev. Physiol. 72,* 579-603.

[31] Zhou, Y. D., Barnard, M., Tian, H., Li, X., Ring, H. Z., Francke, U., Shelton, J., Richardson, J., Russell, D. W., and McKnight, S. L. (1997) Molecular characterization of two mammalian bHLH-PAS domain proteins selectively expressed in the central nervous system. *Proc. Natl. Acad. Sci. U. S. A. 94,* 713-718.

[32] Reick, M., Garcia, J. A., Dudley, C., and McKnight, S. L. (2001) NPAS2: an analog of Clock operative in the mammalian forebrain. *Science 293,* 506-509.

[33] DeBruyne, J. P., Weaver, D. R., and Reppert, S. M. (2007) CLOCK and NPAS2 have overlapping roles in the suprachiasmatic circadian clock. *Nat. Neurosci. 10,* 543-545.

[34] Bertolucci, C., Cavallari, N., Colognesi, I., Aguzzi, J., Chen, Z., Caruso, P., Foa, A., Tosini, G., Bernardi, F., and Pinotti, M. (2008) Evidence for an overlapping role of CLOCK and NPAS2 transcription factors in liver circadian oscillators. *Mol. Cell. Biol. 28,* 3070-3075.

[35] Hogenesch, J. B., Gu, Y. Z., Jain, S., and Bradfield, C. A. (1998) The basic-helix-loop-helix-PAS orphan MOP3 forms transcriptionally active complexes with circadian and hypoxia factors. *Proc. Natl. Acad. Sci. U. S. A. 95,* 5474-5479.

[36] Koike, N., Yoo, S. H., Huang, H. C., Kumar, V., Lee, C., Kim, T. K., and Takahashi, J. S. (2012) Transcriptional architecture and chromatin landscape of the core circadian clock in mammals. *Science 338,* 349-354.

[37] Dudley C.A., Erbel-Sieler C., Estill S.J., Reick M., Franken P., Pitts S., McKnight S.L. (2003) Altered patterns of sleep and behavioral adaptability in NPAS2-deficient mice. *Science 301,* 379-383.

[38] Hoffman, A. E., Zheng, T., Ba, Y., and Zhu, Y. (2008) The circadian gene NPAS2, a putative tumor suppressor, is involved in DNA damage response. *Mol. Cancer Res. 6,* 1461-1468.

[39] Englund, A., Kovanen, L., Saarikoski, S. T., Haukka, J., Reunanen, A., Aromaa, A., Lonnqvist, J., and Partonen, T. (2009) NPAS2 and PER2 are linked to risk factors of the metabolic syndrome. *J. Circadian Rhythms 7;5,* doi:10.1186/1740-3391-7-5

[40] Yi, C. H., Zheng, T., Leaderer, D., Hoffman, A., and Zhu, Y. (2009) Cancer-related transcriptional targets of the circadian gene *NPAS2* identified by genome-wide ChIP-on-ChIP analysis. *Cancer Lett. 284,* 149-156.

[41] Ferre'-D'Amare A. R., Prendergast G. C., Ziff E. B. and Burley S. K. (1993) Recognition by Max of its cognate DNA through a dimeric b/HLH/Z domain. *Nature 363,* 38-45.

[42] Shimizu T., Toumoto A., Ihara K., Shimizu M., Kyogoku Y., Ogawa N., Oshima Y. and Hakoshima T. (1997) Crystal structure of PHO4 bHLH domain-DNA complex: flanking base recognition. *The EMBO J. 16,* 4689-4697.

[43] Longo A., Guanga G. P. and Rose R. B. (2008) Crystal Structure of E47-NeuroD1/Beta2 bHLH Domain-DNA Complex: Heterodimer Selectivity and DNA Recognition. *Biochemistry 47,* 218-229.

[44] Yoshitane, H., Ozaki, H., Terajima, H., Du, N. H., Suzuki, Y., Fujimori, T., Kosaka, N., Shimba, S., Sugano, S., Takagi, T., Iwasaki, W., and Fukada, Y. (2014) CLOCK-controlled polyphonic regulation of circadian rhythms through canonical and noncanonical E-boxes. *Mol. Cell. Biol. 34,* 1776-1787.

[45] Gilles-Gonzalez M. A. and Gonzalez G. (2004) Signal transduction by heme-containing PAS-domain proteins. *J. Appl. Physiol. 96,* 774-783.

[46] McIntosh B. E., Hogenesch J. B. and Bradfield C. A. (2010) Mammalian Per-Arnt-Sim Proteins in Environmental Adaptation. *Annu. Rev. Physiol. 72,* 625-645.

[47] Dioum E. M., Rutter J., Tuckerman J. R., Gonzalez G., Gilles-Gonzalez M. A. and McKnight S. L. (2002) NPAS2: A Gas-Responsive Transcription Factor. *Science 298,* 2385-2387.

[48] Uchida T., Sato E., Sato A., Sagami I., Shimizu T. and Kitagawa T. (2005) CO-dependent Activity-controlling Mechanism of Heme-containing CO-sensor Protein, Neuronal PAS Domain Protein 2. *J. Biol. Chem. 280,* 21358-21368.

[49] Mukaiyama Y., Uchida T., Sato E., Sasaki A., Sato Y., Igarashi J., Kurokawa H., Sagami I., Kitagawa T. and Shimizu T. (2006) Spectroscopic and DNA-binding characterization of the isolated heme-bound basic helix-loop-helix-PAS-A domain

of neuronal PAS domain protein 2 (NPAS2), a transcription activator protein associated with circadian rhythms. *FEBS. J. 273*, 2528-2539.

[50] Uchida T., Sagami I., Shimizu T., Ishimori K., Kitagawa T. (2012) Effects of bHLH domain on axial coordination of heme in the PAS-A domain of neuronal PAS domain protein 2 (NPAS2): Conversion from His119/Cys170 coordination to His119/His171 coordination. *J. Inorg. Biochem. 108,* 188-195.

[51] Rutter, J., Reick, M., Wu, L. C., and McKnight, S. L. (2001) Regulation of CLOCK and NPAS2 DNA binding by the redox state of NAD cofactors. *Science 293*, 510-514.

[52] Ishida M., Ueha T. and Sagami I. (2008) Effects of mutations in the heme domain on the transcriptional activity and DNA-binding activity of NPAS2. *Biochem. Biophys. Res. Com. 368,* 292-297.

[53] Huang N., Chelliah Y., Shan Y., Taylor C. A., Yoo S-H., Partch C., Green C. B., Zhang H., Takahashi J. S. (2012) Crystal Structure of the Heterodimeric CLOCK:BMAL1 Transcriptional Activator Complex. *Science 337,* 189-194.

[54] Wang Z., Wu Y., Li L., Su XD. (2012) Intermolecular recognition revealed by the complex structure of human CLOCK-BMAL1 basic helix-loop-helix domains with E-box DNA. *Cell Res. 170,* 1038.

[55] Doi M., Hirayama J., and Sassone-Corsi P. (2006) Circadian Regulator CLOCK Is a Histone Acetyltransferase. *Cell 125,* 497-508.

[56] Curtis A. M., Seo S. B., Westgate E. J., Rudic R. D., Smyth E. M., Chakravarti D., FitzGerald G. A., and McNamara P. (2004) Histone Acetyltransferase-dependent Chromatin Remodeling and the Vascular Clock. *J. Biol. Chem. 279,* 7091-7097.

[57] Kon, N., Hirota, T., Kawamoto, T., Kato, Y., Tsubota, T., and Fukada, Y. (2008) Activation of TGF-β/activin signalling resets the circadian clock through rapid induction of Dec1 transcripts. *Nat. Cell Biol. 10,* 1463-1469.

[58] Lee, S. K., Achieng, E., Maddox, C., Chen, S. C., Iuvone, M., and Fukuhara, C. (2011) Extracellular low pH affects circadian rhythm expression in human primary fibroblasts. *Biochem. Biophys. Res. Commun. 416,* 337-342.

[59] Madshus, I. H. (1988) Regulation of intracellular pH in eukaryotic cells. *Biochem. J. 250,* 1-8.

[60] Casey, J. R., Grinstein, S., and Orlowski, J. (2010) Sensors and regulators of intracellular pH. *Nat. Rev. Mol. Cell Biol. 11,* 50-61.

[61] Damaghi, M., Wojtkowiak, J. W., and Gillies, R. J. (2013) pH sensing and regulation in cancer. *Front. Physiol. 4;370,* doi:10.3389/fphys.2013.00370

[62] Ichida, S. (2013) Master Thesis.

[63] Chapman-Smith, A., Lutwyche, J. K., and Whitelaw, M. L. (2004) Contribution of the Per/Arnt/Sim (PAS) domains to DNA binding by the basic helix-loop-helix PAS transcriptional regulators. *J. Biol. Chem. 279,* 5353-5362.

[64] Imai, S., Osawa, M., Takeuchi, K., and Shimada, I. (2010) Structural basis underlying the dual gate properties of KcsA. *Proc. Natl. Acad. Sci. U. S. A. 107,* 6216-6221.

[65] Paukert, M., Chen, X., Polleichtner, G., and Schindelin, H. (2008) Candidate amino acids involved in H^+ gating of acid-sensing ion channel 1a. *J. Biol. Chem. 283,* 572-581.

[66] Collier, D. M., Peterson, Z. J., Blokhin, I. O., Benson, C. J., and Snyder, P. M. (2012) Identification of extracellular domain residues required for epithelial Na^+ channel activation by acidic pH. *J. Biol. Chem. 287,* 40907-40914.

[67] Sahlin K., Harris R. C., Hultman E. (1975) Creatine kinase equilibrium and lactate content compared with muscle pH in tissue samples obtained after isometric exercise. *Biochem J. 152,* 173-180.

[68] Ogikubo S., Nakabayashi T., Adachi T., Islam M. S., Yoshizawa T., Kinjyo M., and Ohta N. (2011) Intracellular pH sensing using autofluorescence lifetime microscopy. *J. Phys. Chem. 115,* 10385-10390.

Acknowledgement

I would like to express the deepest gratitude to Dr. Ikuko Sagami, Professor of Kyoto Prefectural University, for her insightful suggestions and enormous encouragements throughout this work.

I am very grateful to Dr. Sumio Ishijima, Associate Professor of Kyoto Prefectural University, for his accurate information and discussions.

I would like to thank all of the members of Cellular Macromolecule Chemistry laboratory for their helpful comments and supports.

Finally, I am grateful to my family for their warm and kind supports.

Never enough
March, 2015
Katsuhiro Yoshii

Publications

Chapter 2

Katsuhiro Yoshii, Sumio Ishijima, Ikuko Sagami. Effects of NAD(P)H and its derivatives on the DNA-binding activity of NPAS2, a mammalian circadian transcription factor. *Biochemical and Biophysical Research Communications* **437** (2013) 386‑391

Chapter 3

Katsuhiro Yoshii, Fumihisa Tajima, Sumio Ishijima, Ikuko Sagami. Changes in pH and NADPH regulate the DNA binding activity of Neuronal PAS domain protein 2, a mammalian circadian transcription factor. *Biochemistry* **54** (2015) 250-259